Science cases – Chapter 1 – Version 3.1 – 30 September 2008

1 Submillimeter observations of galactic star formation (Luca Olmi)

1.1 Submillimeter Galactic Surveys

Dust is the most robust tracer to study the cycling of material from dying stars to the ionized, atomic, and molecular phases of the interstellar medium (ISM), into star forming cloud cores, and back into stars. Atoms, ions, and molecules are imperfect tracers because they undergo complex phase changes, chemical processing, depletions onto grains, and are subject to complex excitation conditions. In contrast, dust is stable in most phases of the ISM; it is optically thin in the FIR over most of the Galaxy, so that its emission and absorption simply depend on emissivity, column density and temperature.

Cold dust in particular (10-40 K) traces the bulk of non-stellar baryonic mass in all of the above phases of the ISM. The temperature and luminosity, and hence mass, of cold dust measured over the entire Galactic Plane (GP) at sub-parsec resolution are the critical observables needed to formulate a global predictive model of the Galactic ISM ⇔ star formation cycling process which drives the Galactic evolution in normal spirals and is a cornerstone for unveiling the formation and evolution of galaxies at different redshifts. The adequate measurement of these key-quantities has been beyond the capabilities of the previous mid to far infrared surveys of the Galactic Plane, either due to limited wavelength coverage or inadequate spatial resolution. In fact, previous surveys such as IRAS, COBE, ISO, Spitzer, Akari have had limited spatial resolution, lack of comprehensive wavelength and/or spatial coverage, poor sensitivity (per pixel), or severe saturation problems. Planned future facilities will have limited wavelength and spatial coverage (e.g. SCUBA-2; SOFIA), small fields of view (e.g. ALMA, JWST, and space borne interferometers) or relatively small angular resolution (e.g., Herschel).

Galactic Surveys fall roughly into 4 categories:

• Galactic Plane surveys (e.g., Herschel Hi-GAL survey)

• Surveys of Giant Molecular clouds (e.g., Herschel Gould Belt survey)

• More specialized surveys (e.g. Debris disks)

• "All-Sky" surveys (e.g., IRAS)

Several (sub)mm to FIR Galactic surveys are currently being carried out, and after Herschel and SCUBA-2 on JCMT will become operational, many more will be completed. BOLOCAM (at 1.1 mm) has already surveyed more than 150 deg^2 of the GP and the ATLASGAL survey using LABOCA on the APEX telescope will survey a few 100s deg^2 of the GP at 870 micron. The BLAST experiment has successfully mapped about 50 deg^2 toward the Vela region and, although shallower, about 200 deg^2 of the GP at 250, 350 and 500 μm (i.e., the same wavebands as the SPIRE instrument on Herschel). Much wider areas will be covered with Herschel and SCUBA-2.

The BLAST experiment, in particular, has demonstrated the importance of mapping the GP at wavelengths near the peak of the cold dust emission. In fact BLAST, until Herschel will be launched, is unique in its ability to detect and characterize cold dust emission from a range of pre- and proto-stellar sources, constraining the temperatures of objects with $T < 25K$ using its three-band photometry near the peak of the spectrum. Previous studies, as those mentioned earlier which do not sample the spectral peak of the thermal emission, have been limited by their relative inability to measure the temperature, producing large uncertainties in the derived luminosities and masses.

Cold interstellar cores lack an internal source of radiation and thus emit the bulk of their radiation at submm wavelengths. Since this emission is optically thin in the submm band, observed flux densities are proportional to column density and mass. There is a variety of terminology used for these elusive early stages, but they are usually called high-mass proto-stellar objects (HMPOs), i.e. compact sources residing in dense molecular clouds, that have the potential to form (one or more) massive OB stars, having luminosities in the range $L \sim 10^2 – 10^5\ L_\odot$, but without associated radio continuum emission.

Recent surveys with Spitzer MIPS can constrain the temperatures of warmer objects (Carey et al. 2005), but the youngest and coldest objects are potentially not detected even in the long-wavelength Spitzer bands. BLAST sources with no associated IRAS or MSX source are potential precluster clumps where no luminous stars have yet formed, demonstrating the ability of BLAST to detect the coldest dust and gas cores in the ISM where star formation has yet to initiate. An example of such source with no MIR counterpart is shown in **Fig.1.1**. To detect and study such cold cores is absolutely fundamental to observe them in wavebands near ~ 200 μm.

In summary, SCUBA2, LABOCA, BLAST and *Herschel* GP surveys will identify pretty much all the massive SFRs in the Galaxy. At the pre- and proto-cluster level (0.1-0.2 pc) we will be pretty much complete to a mass sensitivity of ~ few up to 10s $M_\odot$ and with SEDs in the range ~70 - 850 μm. These data will be also combined with high resolution IR data from Spitzer, VLT, etc, plus mm/sub-mm/radio-waves surveys from CARMA, PdBI, VLA, ALMA, etc.

Many of these regions will be followed up with molecular line surveys. However, only a few (sub)mm heterodyne array receivers exist so far, such as: HARP@JCMT, a 16-pixel array receiver at 0.8mm; HERA@IRAM, a 2, 3x3-pixel array receiver at 1.1mm; PACS@*Herschel*, a 5x5-pixel array at 55-210 micron, but with low-spectral resolution.

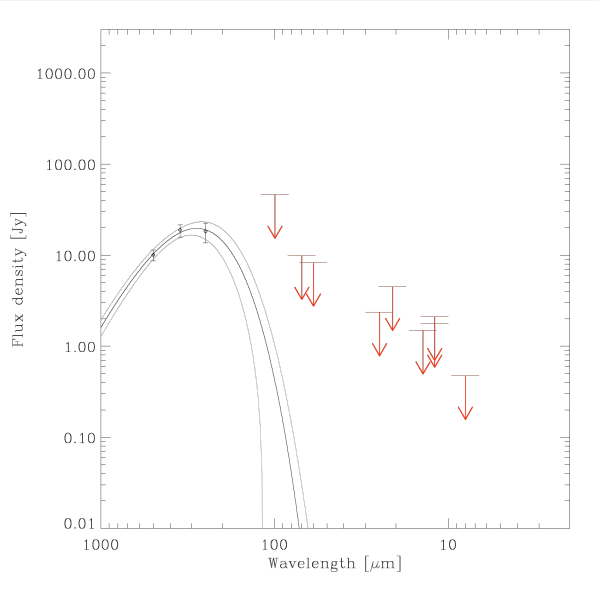

Figure 1.1 The SED of the coldest BLAST source in the Vulpecula region (V11, T=10 K). The FIR spectrum turns over in the BLAST bands (from Chapin et al. 2008).

1.2 Science drivers for submm galactic surveys: Low- and Intermediate-Mass SF

1.2.1 Open questions

The process of low- to intermediate-mass star formation is now reasonably well known. However, the earliest phases of SF still remain poorly understood. Thus, the general motivations for extensive galactic surveys of the GP are the following:

- What determines the distribution of stellar masses at birth (IMF)?
- How are pre-stellar cores created in molecular clouds and what governs their evolution to proto-stars ?
- On the scale of a GMC, is star formation generally a slow process (taking several dynamical times and mediated by ambipolar diffusion) or a fast, dynamic process (mediated by turbulent fragmentation)?
- Are the initial cloud conditions required for the "clustered mode" of star formation fundamentally different from those of the "isolated mode" ?

While surveys with BLAST and *Herschel* are sensitive enough to address many of these issues, it is doubtful that they will have the required angular resolution to determine the cores' mass and temperature internal distribution, even in the nearest clouds. In fact, the ~15 arcsec angular resolution of Herschel around ~200 μm is adequate to achieve a complete census of cold cores and for probing individual (0.01-0.1 pc) star-forming cores up to a distance of 0.5 kpc. However, *Herschel* angular resolution is just barely enough to probe the most internal regions of pre-stellar cores, which may be significantly colder (with T as low as ~5–7 K) than in their outer parts. At such low temperatures observing at wavelengths >~200 μm is absolutely critical, and therefore the higher angular resolution of the PACS instrument on *Herschel* becomes less relevant when compared with ground instruments.

requires high angular resolution, is confusion due to source clustering. Most of low- and intermediate-mass SF takes place in crowded regions where the ability to spatially resolve nearby sources in similar or very different evolutionary phases is critical to identify the sources and construct their Spectral Energy Density (SED) function.

1.2.2 Simulation of high-mass cores

The importance of observing at 200 μm at higher angular resolution is shown in **Fig. 1.2**, where we present the results of the simulation of two nearby high-mass cores, assumed to be at a distance of 3.2 kpc. On the top panel of **Fig. 1.2** the 200 micron maps are presented, whereas the 350 micron maps are shown in the lower panel. The core at the center of the map is an isothermal early core at T=12 K, with the radius of the densest region being 0.05 pc and with a decreasing column density from the core center. The source on the top-right has instead a negative temperature gradient outward, in addition to a decreasing column density, with a central radius of 0.02 pc and T=15 K. A separation of about 5.7 arcsec (about 0.1 pc) has been taken between the two sources. Noise has been added to be consistent with ASO and CCAT (see **Tab. 1.1**), and the FOV (filled with bolometers) of ASO has been assumed to be twice that of CCAT.

	ASO@200 μm	CCAT@200 μm	ASO@350 μm	CCAT@350 μm
NEFD [mJy √s /beam]	480	157	56	17
1-σ, 1-hr sensitivity [mJy/beam]	8	2.6	0.9	0.3
τ_o	2.0	2.2	0.4	0.5

Table 1.1 Main parameters used for the simulation shown in Fig. 1.3. τ_o is the optical depth at the zenith.

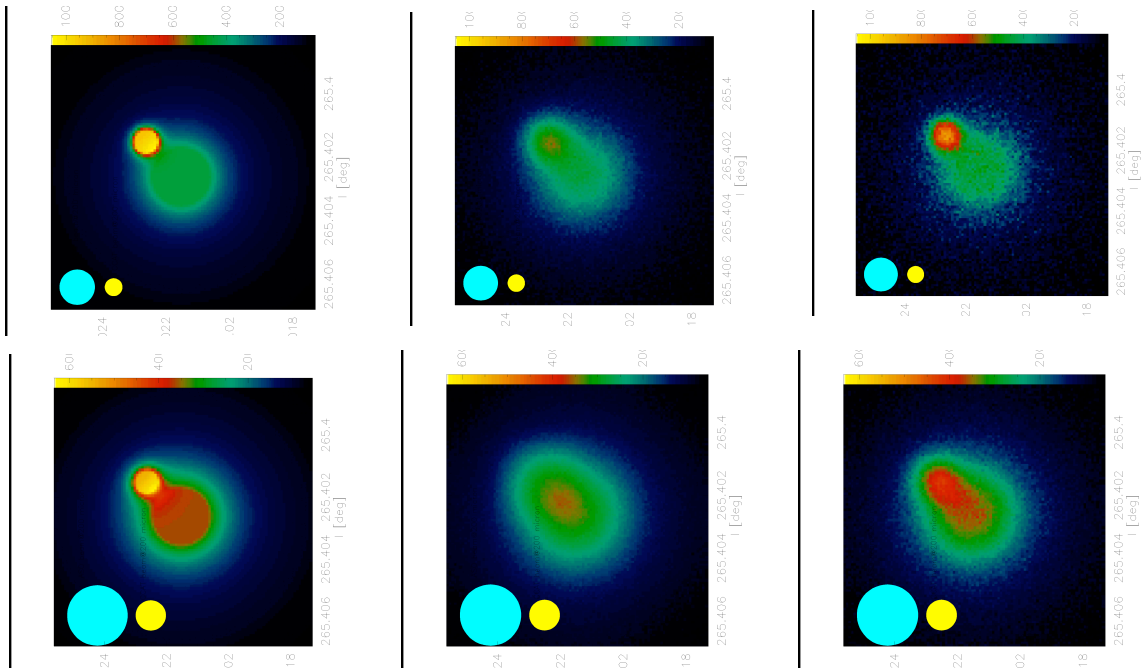

Figure 1.2 Simulation of two nearby high-mass cores (assumes optically thin emission): **Top**: model source emission at 200 μm (left), 200 μm ASO map (middle), and 200 μm CCAT map (right). **Bottom**: same as above at 350 μm. The maps are 30 arcsec wide and each pixel is 0.3 arcsec. The light-blue and yellow discs correspond to the FWHM of the ASO and CCAT beams, respectively.

This is causing the slightly larger granulosity in the CCAT maps, where each point is sampled for less time. Appropriate observing conditions have been assumed at each site, i. e., drier conditions for shorter wavelengths; an elevation of 60° and the same amout of mapping time have been assumed for both telescopes.

It is important to note that the only way to reach unambiguous conclusions on the core structure, thus setting constraints on the theoretical models describing the initial conditions for individual protostellar collapse, is to reconstruct the temperature and column-density profiles simultaneously through multi-band imaging (at wavelengths longward of ~200 μm). Ground observations are invaluable to achieve the required angular resolution. Another important potential issue in cluster-forming regions, that

We can clearly see the effects of angular resolution. At 200 micron, the two nearby cores are clearly separated in the CCAT simulated map, and are barely resolved in the ASO map (ASO – Antarctic Submillimeter Observatory, an ALMA-like 12m antenna). However, at 350 micron, ASO is no longer able to separate the two cores, which are seen as a single object instead. The advantage of the larger CCAT diameter is quite evident in this specific example. However, the noise in the maps, expressed as MJy/srad, are quite similar due to the larger ASO beam, and the mapping speed is higher with ASO.

1.3 Science drivers for submillimeter galactic surveys: High-Mass SF

Like LMS, HMS (i.e., M >~ 8 $M_{\odot}$) form in dense cores within molecular cloud complexes. Unlike LMS, however, massive young stellar objects reach the zero-age main sequence while still deeply embedded and accreting their final masses. Thus, at this stage the copious UV flux emitted by the central massive star creates a HII region which is expected to slow down and halt the accretion of cloud material (e.g., Stahler et al. 2000). This is clearly a specific theoretical problem, and to solve it two competing families of models have been proposed: accretion (with high accretion rates or

channeled through a disk; e.g., McKee & Tan 2003, Yorke & Sonnhalter 2002) versus coalescence of several lower-mass protostars (e.g., Bonnell et al. 2001).

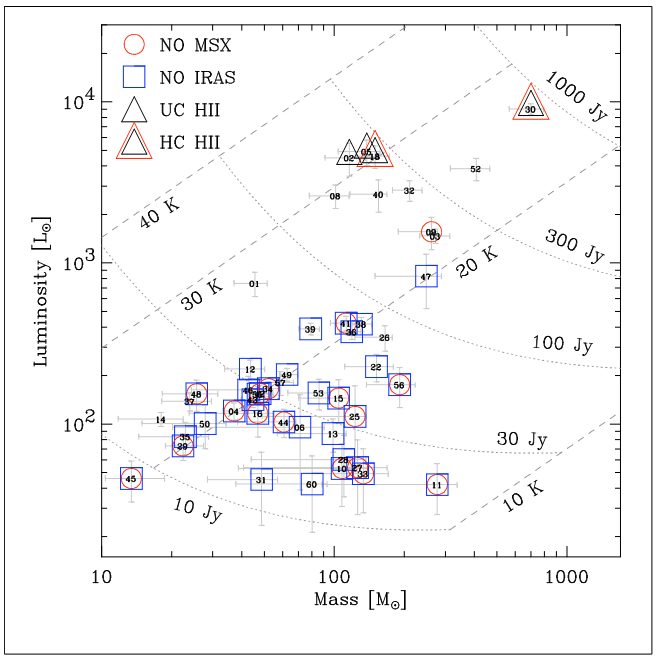

Figure 1.3 Luminosity vs. mass for the 49 objects observed by BLAST05 toward the Vulpecula region and believed to be associated with NGC 6823 (Chapin et al. 2008).

Observationally, once young massive stars have developed an ultracompact HII (UCHII) region, they can be easily detected in the IR and radio centimeter continuum. However, earlier stages of massive SF, i.e. pre-stellar, are best detected via FIR or (sub)millimeter dust continuum. Several candidate massive protostars have been identified as IRAS sources (e.g., Molinari et al. 2000; Beuther et al. 2002), but HMPOs are colder and hence very weakly emitting in the MIR bands of IRAS, MSX or Spitzer. The survey of the Vulpecula region by BLAST during its 2005 flight has clearly shown the ability of FIR/submm observations to identify many new HMPO candidates (Chapin et al. 2008), which are shown as objects without a MIR counterpart in **Fig. 1.3**.

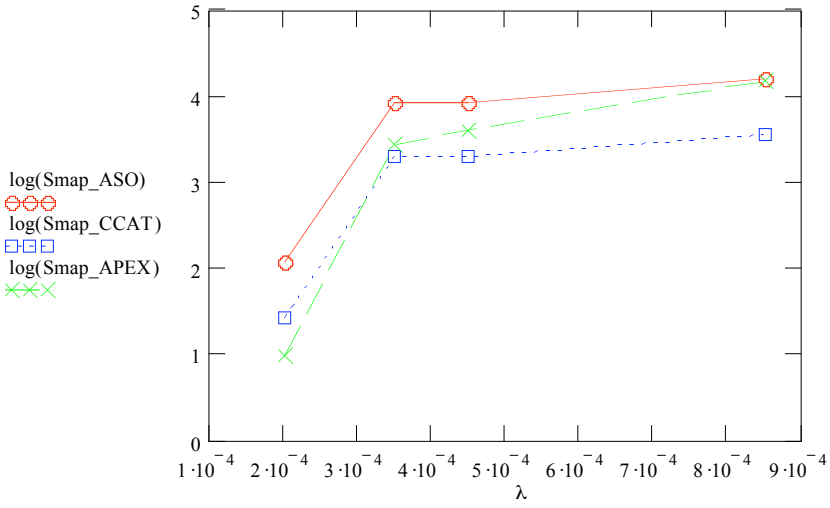

Figure 1.4 Log of mapping speed (in arcmin^2/hr), achieving a 10mJy/beam sensitivity on point sources, vs. wavelength (in m) for the ASO, CCAT and APEX telescopes.

Since the earliest phases of high-mass star formation (young protostars and especially HMPOs) have been studied in very few objects up to now, the initial conditions of this process remain poorly known. Also very schematic remains our knowledge of what are the characteristics of molecular cloud complexes in terms of temperature, density, and velocity structure, as well as non-thermal support and degree of fragmentation, that may affect the process of HMSF.

1.4 Comparison with other facilities

1.4.1 Mapping speed

The higher-angular resolution coupled with a large field of view at the shortest wavelengths is the biggest driver for ground telescopes, as compared to (sub)orbital facilities. Though many Galactic and Extra-Galactic surveys will already be completed by the time a facility at Dome C might be operational, mapping speed will still be an important parameter to compare telescope performance.

In **Fig. 1.4** we thus compare the mapping speed of the ASO, CCAT and APEX telescopes at four different wavelengths. In this comparison we always assume average transparency conditions (as given in Table 1) and also assume that the bolometer arrays have the same properties at the different telescopes. We also scale the number of pixels with wavelength, so that there are less pixels in the array at longer wavelengths. As a consequence, the FOV at different wavebands and for different telescope is *not* the same, as it depends on the telescope beam and number of pixels in the array. Despite ASO and APEX have the same telescope aperture (and thus beam FWHM) we note that the mapping speed of ASO is always better than that of CCAT, due to marginally better transparency *and* especially the larger beam. ASO and APEX achieve the same mapping speed only somewhere near the 850 µm waveband.

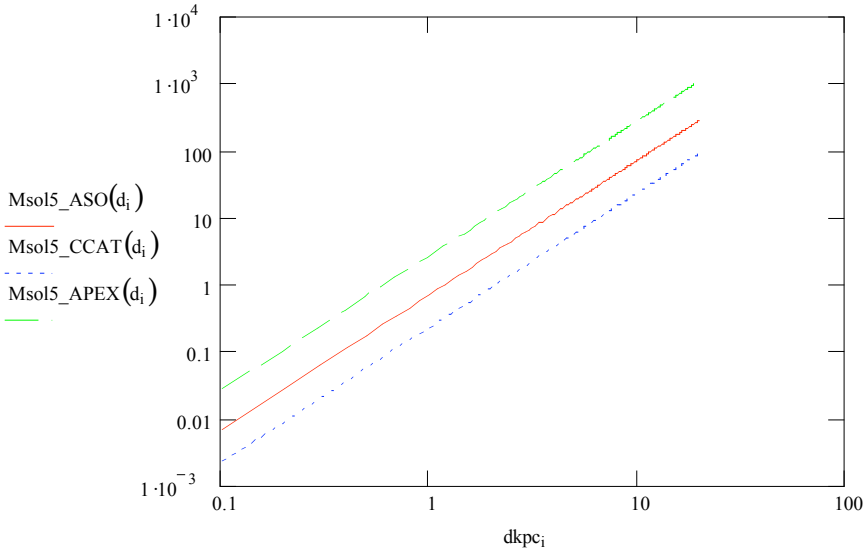

Figure 1.5 Log-log plot of the 5-sigma mass limit (in solar masses) achievable in 1-hr, at 200 µm, vs. source distance (in kpc) for the ASO, CCAT and APEX telescopes.

1.4.2 Mass sensitivity

Likewise, the mass sensitivity (for Galactic observations) is another important parameter to compare different facilities. In **Fig. 1.5** we compare the 5-sigma mass limit at 200 µm (for 1-hr integration), for the ASO, CCAT and APEX telescopes, as a function of source distance. The comparison is done at the shortest wavelength because that is where the higher-angular resolution is achieved. We note that there is a factor of about 4 in sensitivity difference between ASO and APEX and a factor of 3 between ASO and the much larger CCAT. We also see that within 1 kpc distance the mass sensitivity of CCAT

is at most slightly larger than 0.1 $M_\odot$, whereas ASO sensitivity in 1-hr approaches 1 $M_\odot$ at 1 kpc. This is an important factor when planning surveys which must be *complete* in terms of core detection. For HMSF regions at distances between 1 and 10 kpc it will be difficult for both CCAT and ASO to achieve deep maps without long integration times. It will also be much more difficult for APEX and likely to be impractical to achieve complete surveys at distance >~ 1 kpc.

1.4.3 Transparency

Finally, we estimate what would be the required transparency at Dome C to achieve a point source sensitivity equal to that of CCAT. In **Fig. 1.6** we show the optical depth at the zenith, τ_o, as a function of the parameter f = NEFD(ASO) / NEFD(CCAT), using as a parameter the surface RMS of ASO in micron. We note that using the nominal $\tau_o \approx 2$ at 200 micron at Dome C, NEFD(ASO) is almost 3.6 times that of CCAT, assuming a nominal 12 micron surface RMS. Even for a much better surface at 6 micron RMS, f is still about 2.5. The situation changes if τ_o is smaller, e.g. like for Dome A where $\tau_o \approx 1$ at 200 micron. In this case a 12m antenna with a 10 micron RMS surface would achieve about the same NEFD as CCAT (f ≈1).

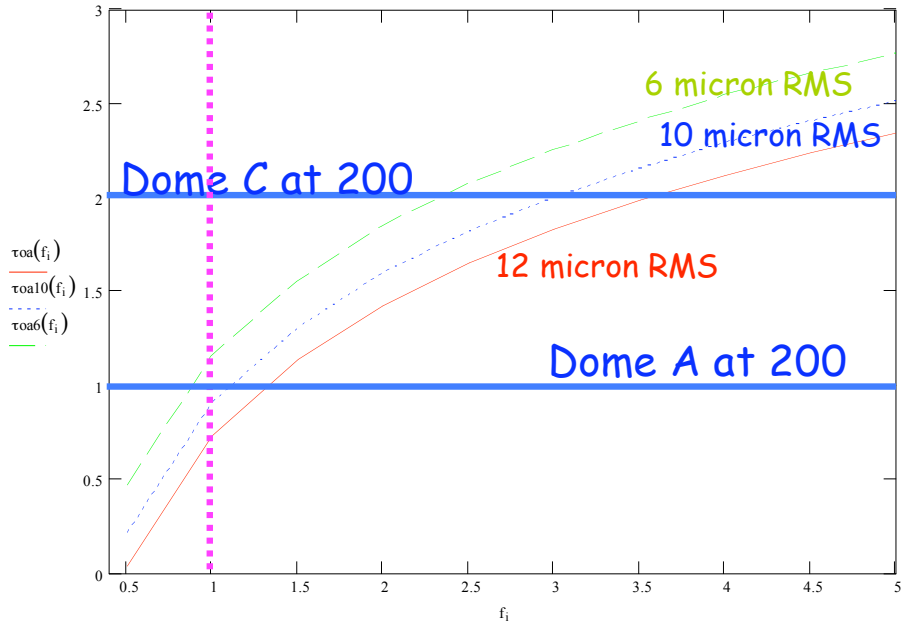

Figure 1.6 Zenith optical depth at 200 micron (*y*-axis) required to achieve a given factor f=NEFD(ASO)/NEFD(CCAT) (on the *x*-axis), for various surface RMS. The vertical dashed line indicates where ASO and CCAT would have the same NEFD.

1.5 Conclusions

Given the present and near-future status of large-scale, dust continuum surveys, the largest massive star formation driver for a submm telescope able to operate in the THz regime is arcsec resolution in the 200 micron window. Also, atomic and molecular line surveys of SFRs are still in their infancy, and most of the (sub)orbital experiments will use arrays with low-spectral resolution. This would potentially constitute a strong driver for a large Antarctic antenna, assuming such an array receiver is technically feasible.

References

Beuther, H., Schilke, P., Menten, K. M., Motte, F., Sridharan, T. K., Wyrowski, F. 2002, ApJ, 566, 945

Bonnell, I. A., Bate, M. R., Clarke, C. J., Pringle, J. E. 2001, MNRAS, 323, 794
Carey, S. J., et al., 2005, in Bulletin of the American Astronomical Society, 1252
Chapin E., et al., 2008, ApJ, 681, 428
McKee, C. F., Tan, J. C. 2003, ApJ, 585, 850
Molinari, S., Brand, J., Cesaroni, R., Palla, F. 2000, A&A, 355, 617
Stahler, S. W., Palla, F., Ho, P. T. P. 2000, in Protostars & Planets IV, 327
Truch M., et al., 2008, ApJ, 681, 415
Yorke, H. W., Sonnhalter, C. 2002, ApJ, 569, 846

2 **Spectral lines and the interstellar medium** (Carsten Kramer)

A 12m telescope at Dome C will open the realm of submillimeter observations at high angular and spectral resolutions from Antarctica. The excellent atmospheric transmission from Dome A will allow routine observations in the 450 and 350 µm atmospheric windows. Under exceptionally good conditions, the THz windows between 300 and 200 µm become accessible. Dome C will allow for routine spectroscopic observations of several key species of the ISM.

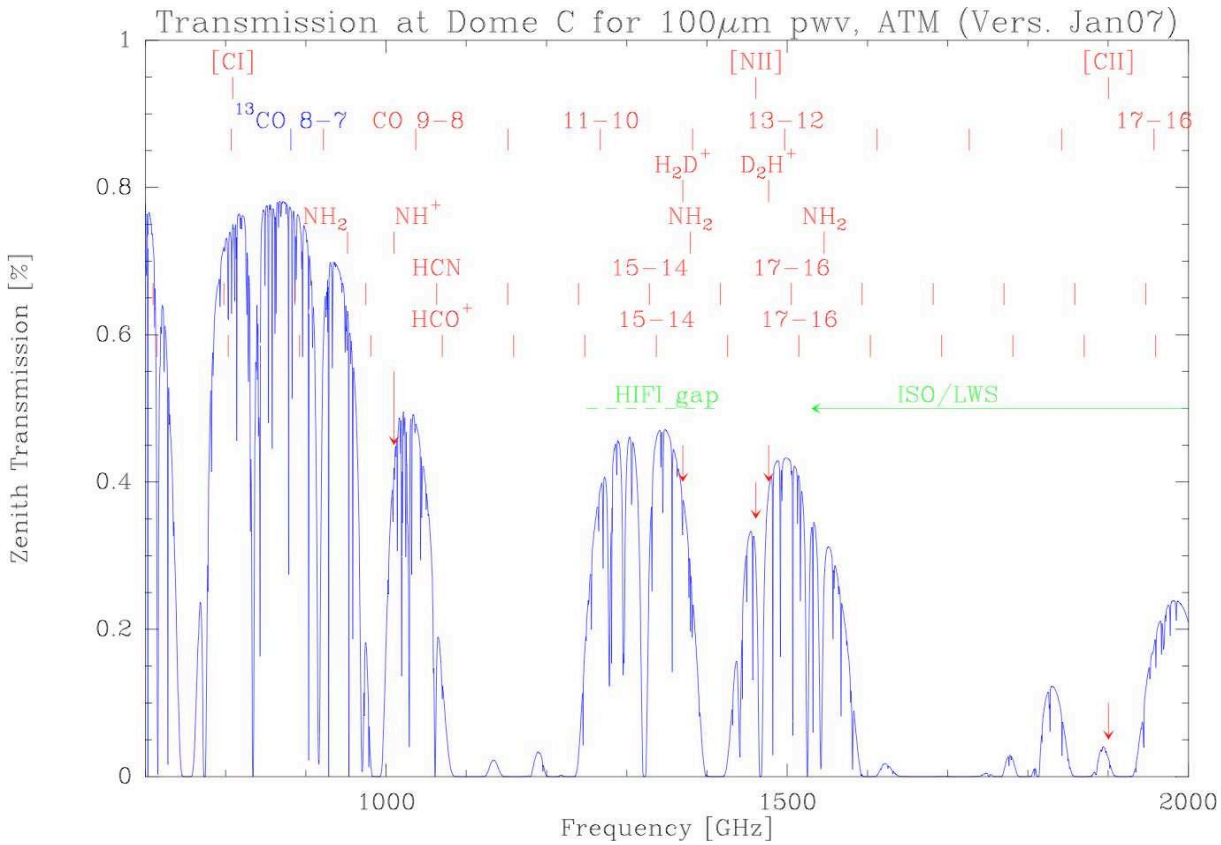

Figure 2.1 Atmospheric transmission and a few key spectral lines of the ISM between 700 GHz and 2 THz. The atmospheric windows centered near 350 µm (860 GHz), 290 µm (1050 GHz), 230 µm (1300 GHz), and 200 µm (1500 GHz) are clearly visible. The transmission curve was calculated using ATM (J. Pardo) for Dome C altitude assuming excellent atmospheric conditions, i.e. 100 µm precipitable water vapour (pwv) (cf. the FTS spectrum obtained at 93 µm pwv at Cerro Sairecabur by Marrone et al. 2005).

Existing frequency surveys of e.g. the Orion KL star formation region in the submillimeter windows show a plethora of species and the great potential of a 12m telescope at Dome C for studying the chemistry of the ISM. Important tracers of the dense, warm molecular gas tracing the immediate neighboorhood of star formation, are the high-rotational lines of CO, HCN, HCO+. Among the most important spectral lines, is the NII line at 205 μm line which will allow to study the distribution and kinematics of the ionized gas. Studying the ground-state rotational transitions of deuterated H3+ will significantly improve our understanding on the orchestry of the chemical network in the ISM, and in particular in dense, molecular cloud cores, the future sites of star formation.

2.1 Atmospheric conditions and competing observatories

The Terahertz windows are only accessible under exceptional weather conditions from Dome C. The bulk of science observations will therefore be restricted to wavelengths longer than 350micron, i.e. frequencies of less than 880 GHz. Radiosounding analysis indicates that at Dome C, 25% of the time PWV=0.23 mm and 50% of time PWV=0.33 mm. The resulting atmospheric transmission for 0.3 mm pwv is about 50% in the atmospheric windows near 450 μm and 350 μm, but drops to less than 10% in the windows at shorter wavelengths. For 0.2 mm pwv, the THz windows have transmission of about 15%. Note however that despite these discouraging predictions, Oberst et al. (2006) recently succeeded to map the NII(205 μm) line from the South Pole in a Galactic star forming region. It should be noted that Dome A is possibly the vastly superior site on Antarctica (Storey, Burton et al.). A 12m telescope at Dome A may therefore open the THz windows for routine observations. Building a remotely operated and transportable 12m telescope at Dome C may be a sensible first step before going to Dome A. The half power beamwidths of the 12m dish at 806 and 460 GHz will be 8" and 13", similar to those of the 12m-APEX telescope. Competing instruments, which will also study spectral line emission of the ISM in the 450 and 350 μm windows, are the 12m-APEX telescope at 5100m altitude on the ALMA site. ALMA will eventually observe at these submillimetre wavelengths. Heterodyne submillimetre instruments are also planned for the 25m-Cornell Caltech Atacama telescope (CCAT) which is under serious consideration for the 5612m site on top of Chajnantor. The airborne and spaceborne 3m-class observatories SOFIA and Herschel will be able to observe at these frequencies. However, their wavelength coverage is much larger and these observatories will naturally focus on observations in the far-infrared, inaccessible from the ground.

2.2 The science case

2.2.1 The dense, warm gas traced by CO, HCN, HCO+

High rotational transitions of CO, HCN, HCO^+ allow to trace the density and temperature structure of the warm and dense gas found in the immediate neighbourhood of active star formation sites, e.g. hot cores and photon dominated regions.

The rotational ladder of the chemically very stable molecule CO allows to trace a wide range of excitation conditions depending on the rotational transition J: the upper energy level is 2.8 J (J+1) Kelvin and the critical density is $4x10^3$ J^3/cm^3. The CO 13--12 transition lying in the 200 μm window for example is only excited in warm and dense gas, as it has an upper energy level of 510 K and a critical density of 10^7 cm^{-3}.

While KAO and ISO observed integrated intensities of high-J, i.e.THz, CO lines with resolutions of about an arcminute, only few velocity resolved observations of these lines exist to date: Pioneering work was conducted by Boreiko & Betz (1989, 1991, 1997) who used their heterodyne experiment on-board the KAO to observe THz CO lines. THz CO lines were later observed in a few sources by Marrone et al. (2004, 2005) using the 0.8m RLT, by Kawamura et al. (2002) using the 10m HHT, and by Wiedner et al. (2006) using CONDOR at the 12m APEX telescope. The optically thin ^{13}CO(8-7) line at 880 GHz is also accessible from the ground, providing the rare opportunity to obtain direct measures of the column densities of the warm and dense gas (e.g. Kramer et al. 2004, Wyrowski et al. 2006 using the KOSMA 3m and the APEX 12m telescopes).

Due to their large dipole moments, THz transitions of HCN and HCO^+ trace very high densities and excitation conditions. The Orion KL frequency survey in the 350-µm window by Comito et al. (2005) using the CSO shows very strong HCN and HCO^+ lines of between 30 and 100 K main beam temperatures. Comito et al. detected a total of 26 species tracing the very rich hot core chemistry. High excitation transitions of CH_3OH, CH_3CN, H_2CO, HNCO, and C_2H_5CN indicate the presence of a very hot (~250 K) component. SO_2 and CH_3OH are the main coolants, not CO.

2.2.2 Phase-structure of the ISM and the NII 205-µm line

Heterodyne observations of the bright, but so-far largely unexplored NII 205-µm line allows to study the distribution and kinematics of the warm, low-density ionized gas and is hence an excellent, extinction free probe of star formation. The relative importance of the various ISM phases will be disentangled by comparing NII, CII(158 µm), HI, CO line profiles tracing the ionized, atomic, and molecular medium.

Only few observations of the NII(205 µm) line exist to-date: Colgan et al. (1993) observed both NII fine-structure lines in G333.6-0.2 with the KAO. FIRAS/COBE was used to map the entire Milky Way at ~8° resolution showing that the 205-µm line is a very strong Galactic FIR cooling line, second only after CII at wavelengths beyond 100 µm. Oberst et al. (2006) detected the 205 µm line in the Carina I HII region from the South Pole using SPIFI at the former AST/RO 1.7m submillimeter telescope.

The phases of the ISM are characterized by the ionization state of hydrogen: HII and HI regions, and molecular H_2 clouds. HII regions comprise dense HII regions in the vicinity of OB stars, the diffuse warm ionized medium (WIM), and a hot phase (HIM). HI regions comprise the warm and the cold neutral medium (WNM, CNM) (McKee & Ostriker 1977; Cox 2005).

The NII 205-µm line has nearly the same critical density as the CII 158-µm line for electron impact excitation. The critical densities are 44 cm^{-3} for the 205-µm line and 293 cm^{-3} for the 122-µm line, for an electron temperature of 8000 K. However, N^+ takes 14.5 eV to form, so that (unlike C^+) it is only found in ionized gas regions. Therefore, the line ratio in ionized media is essentially only a function of the N^+/C^+ abundance ratio - which is not sensitive to the hardness of the stellar radiation fields since it takes about the same energy to form N^{++} as it does to form C^{++}. Oberst et al. (2006) have used this technique to deduce that 27% of the observed CII emission from the Carina Nebula arises from the diffuse ionized gas (the rest arising from photon dominated regions (PDRs)). The 122-µm NII line has been used in a similar fashion (Kramer et al. 2005, Contursi et al. 2002) to show that up to 30% of the CII observed with ISO/LWS in the spiral arms of M83 and M51 stem from the ionized phase. However, studies with the 122-µm line, are compromised by the density dependence of the NII 122 µm CII ratio - an effect greatly mitigated by using the 205-µm NII line. Supplementing FIR lines tracing the high density ionized gas are e.g. the OIII lines at 88 and 52 µm.

NII is an excellent, extinction free tracer of star formation. In contrast to the radio continuum, which is emitted by thermal and non-thermal processes, which are difficult to separate, NII emission is not polluted by nonthermal radiation. Calzetti (2007) recently suggested using a combination of 24micron emission obtained with Spitzer and Hemission as tracer of the star formation rate. These two tracers probe both, the dust obscured and unobscured star formation. The proposed observations of NII will provide an excellent independent test of this approach.

2.2.3 Prestellar cores and deuterated species

H^{3+} is a key species in the chemical network at play in the ISM. However, it is observationally accessible only via infrared absorption spectroscopy. In prestellar cores, H^{3+} is one of the very few

molecules expected to stay in the gas-phase, when almost all C,N,O bearing molecular species have frozen-out on dust grains.

Spectroscopic observations of the isotopomers of H^{3+} should therefore in principle allow to trace the kinematics in the inner, cold, dense prestellar cores, before the onset of star formation. Very high deuteration levels have been observed in prestellar cores, allowing to use H_2D^+ and D_2H^+ to study their physica conditions (Walmsley et al. 2004, Flower et al. 2004). Note that D^{3+} lacks any dipole moment, similar to H^{3+}, and can thus only be detected via absorption studies in the NIR.
The ortho- H_2D^+ ground-state transition at 372 GHz has been detected in dark clouds, but also towards low-mass protostars and in protoplanetary disks (Stark et al. 1999, 2004, Vastel et al. 2004, Harju et al. 2006, Ceccarelli et al. 2004). However, the ground-state transition of para- H_2D^+ at 1370 GHz has not been detected yet despite several attempts (Philips et al. 1985, Boreiko & Betz 1993). It is noteworthy that this transition was lying outside the ISO/LWS wavelength range and will also lie outside the HIFI/Herschel tuning range. The situtation is similar for D_2H^+. The para-D_2H^+ ground-state line at 692 GHz has been detected by Vastel et al. (2004) in the core of 16293E, the ortho- D_2H^+ line at 1477 GHz has not been detected yet.

2.2.4 References

Boreiko & Betz 1989
Boreiko & Betz 1991
Boreiko & Betz 1993
Boreiko & Betz 1997
Calzetti 2007
Ceccarelli et al. 2004
Cernicharo et al. 1996
Colgan et al. 1993
Comito et al. 2005
Contursi et al. 2002
Cox et al. 2005
Flower et al. 2004
Harju et al. 2006
Kawamura et al. 2002
Kramer et al. 2004
Kramer et al. 2005
Marrone et al. 2004
Marrone et al. 2005
McKee \& Ostriker 1977
Oberst et al. 2006
Philips et al. 1985
Stark et al. 1999
Stark et al. 2004
Vastel et al. 2004
Walmsley et al. 2004
Wiedner et al. 2006
Wyrowski et al. 2006

3 Magellanic cloud (Frank Israel)

3.1 Dust: a major ISM component

Dust particles are an important component of the interstellar medium. They shield fragile molecules such as CO from destruction by UV photons, and they allow other molecules such as H_2 to form by grain-surface reactions. Dust grain populations are the outcome of local conditions, such as metallicity and energetics. For instance, shocks from expanding SNRs are a major and efficient source of dust particle erosion and destruction on short timescales (Jones et al. 1994, 1996). This rapid erosion may

be countered by efficient accretion of dust particles in quiescent, dense (molecular) gas clouds. Several authors have attempted to extract the resulting equilibrium particle size distribition from measurements of Solar-Neighbourhood objects (e.g. Mathis et al 1977). At the small end of their distribution, hot very small grains excited by the absorption of a single photon (Draine & Anderson, 1985) and even smaller PAHs (Léger & Puget 1984) occur. Including these additional populations, Weingartner & Draine (2001) constructed metallicity-dependent size distributions for carbonaceous and silicate grains pertinent to the different conditions in the Galaxy, the LMC and the SMC and other physically-based dust emission models are also becoming available (e.g. Li & Draine 2001; Zubko et al. 2003).

As the erosion timescales are short compared to accretion timescales, variations in ambient conditions may rapidly and substantially alter local grain size distributions. Alteration of the balance between big grains and very small grains may cause noticeable changes in SED shapes. This appears to be the case in the strong starburst environment characterizing the dwarf galaxy NGC 1569 (Lisenfeld et al. 2002). A small but clear emission excess at submillimeter wavelengths is unlikely to be caused by cold `classical' big grains. Rather, most of the submillimeter and far-infrared emission from this galaxy appears to originate in very small grains with a relatively small total mass. Thus, in environments with extensive dust grain processing, traditional interpretations easily overestimate dust masses, and consequently underestimate both gas-to-dust ratios and gas masses deduced from dust emission.

Even if this interpretation were not correct, models still need to take into account some form of very cold dust, particularly in regions of low metallicity. For instance, 'very cold' dust emission has also been found in NGC 4631 (Dumke et al. 2004), in Virgo blue compact dwarf galaxies (Popescu et al. 2002) and in the MW itself (Reach et al. 1995). Other explanations invoke fractal dust aggregates or diffuse non ionizing UV radiation. The difficulty in interpreting the local 'very cold' emission is our lack of absolute submm measurements within the MW, and the difficulty in extragalactic studies is the lack of spatial resolution and hence wide range of temperatures within the beam.

As a major part of the astration cycle, the ISM plays an essential role in galaxy evolution. It is thus important to gain insight in the processes that govern dust grain processing and dust particle size distributions. Studying far-infrared/submillimeter SEDs as a function of varying ambient conditions is a very promising way of making significant progress.

3.2 The Magellanic Clouds: ideal astrophysical laboratories.

The closest Milky Way satellites, the Large Magellanic Cloud (LMC) and the Small Magellanic Cloud (SMC) provide the ideal astrophysical laboratories for such investigations. With distances of 50 kpc (Feast 1999) and 61 kpc (Keller & Wood 2006) respectively, they are ten times closer than other major systems in the Local Group of galaxies, and typically 40-100 times closer than other `nearby' galaxies. Their external nature but close proximity simultaneously provides full global and unimpeded very detailed views. They allow us to resolve parsec-sized structures, making it possible to study ISM processe unambiguously on scales dominated by a single star. They have low dust and metal abundances, different from each other and from the Milky Way, thus providing three different metallicity baselines.

The LMC, with a metallicity one quarter solar (Dufour et al. 1984), has a mass of 9×10^9 $M_\odot$ (van der Marel et al. 2002), a size of about 8 kpc and a star formation rate of 0.1 $M_\odot$/yr (Whitney et al. 2007). The SMC, with a metallicity one tenth solar (Dufour et al. 1984) has a mass of 2.5×10^9 $M_\odot$, a size of about 3 kpc, and a star formation rate of 0.05 $M_\odot$/yr (Wilke et al. 2003). Metallicities show little variation across either system, but luminous star formation has created a very large range of ambient radiation field intensities in each Cloud. UV radiation field intensities in both Clouds range from less than those in the MW Solar Neighbourhood to hundreds of times higher.

We can therefore study the effects of ambient radiation fields at constant metallicities. Because of

their particular nature, the Magellanic Clouds provide well-determined environments representing a variety of metallicities and energy densities in which the resulting properties of the interstellar medium can be studied in a detailed and systematic manner not offered elsewhere. Not only is by far the largest part of the Milky Way (MW) unaccessible to such studies, but all ISM studies in the MW also greatly suffer from confusion caused by line-of-sight crowding and distance ambiguities. In the LMC and the SMC, everything is essentially at the same distance, and determinations of mass and luminosity are unambiguous and directly comparable. The LMC is particularly favourable because its limited depth and its viewing angle of 35° (van der Marel & Cioni 2001) place only a single cloud along any line of sight.

3.3 A proposed FIR/Submm observing program

At present, no systematic far-infrared/submillimeter survey of either LMC or SMC exists. Shortwards of 200 microns, IRAS and Spitzer maps are available, not allowing, however, to investigate the crucial submillimeter exces. This may become possible, for the first time, if the Herschel Space Observatory mission is succesful. One of its accepted Open Time Key Programmes aims at conducting uniform surveys of the LMC and the SMC in the 250, 350 and 500 micron bands.

Here, we propose to conduct similar surveys of both Clouds in the 200, 350, and 450 micron bands with a 12 m telescope at the best possible site on Earth, providing an order of magnitude more collecting area and more importantly, 3.5 times higher linear resolution. Such resolutions will render the survey sensitive to interstellar conditions on scales of 1-2 parsec, i.e. allows us to distinguish the spheres of influence of individual stars - a feat not possible with the Herschel surveys, even if they are fully succesful. We propose a baseline observing program involving 2300 hours of integration time per band (total observing time can therefore be reduced considerably by simultaneous observation), per Cloud. We have assumed NEFDs of 750 mJy/beam, 150 mJy/beam, and 150 mJy/beam at 20 microns, 350 microns, and 450 microns respectively. For the LMC (8°x8°) this yields sensitivities of 138 MJy/sr, 7.5 MJy/sr and 3.5 MJy/sr, or 45 mJy/beam, 5 mJy/beam, and 4 mJy/beam. For the SMC, the same integration time yields sensitivities 4 times better (because the surface area to be covered is 16 times less than for the LMC). With these numbers, the proposed survey will not only have a significantly better resolution than the expected Herschel maps, but for the LMC also a better sensitivity per (smaller!) beam than Herschel at 350 and 500 microns, and for the SMC even much better sensitivity.

The resulting images will provide unique insight in the conditions dominating dust in the interstellar medium of galaxies. As the measurements cover the Rayleigh-Jeans side of the warm dust emission spectrum, they are relatively little affected by large temperature-related uncertainties, and allow study of the coldest ISM dust. The dust maps will show the distribution of (cool) dust on typical scales of 1-2 parsecs corresponding to typical gas column densities of 10^{21} and 10^{22} H-atoms/cm^2 for the LMC and SMC, respectively. The measurements are similar to those planned for the Herschel SPIRE experiment, but their 3.5 times higher linear resolution (12 times higher area resolution) render them fully complementary to these, and in fact uniquely provide the extremely high linear resolution that is needed to study the effects of stars on their immediately surrounding ISM. The high resolution also will allow even better identification of embbedded young stellar objects (YSOs), as they will now have an order of magnitude higher contrast with theiir surroundings than in the Herschel maps. The variation in dust properties gleaned from the dust maps together with the inventory of radiation sources and gas densities obtained from other already existing datasets will allow us, in particular, to study changes in interstellar grain excitation and size distribution, i.e. follow in detail the process of dust particle erosion in areas dominated by radiation, by shocks, and at significantly different metallicities.

An alternative approach may also be considered, if the Herschel observations are succesful. Instead of duplicating uniform surveys, the resulting maps may be used to select emission regions for deeper integration. Depending on the scope if such a program, the dust emission in both LMC and SMC may then be probed an order of magnitude deeper than in these maps. This is important, because the 12m

observations will then reach low-mass, low-surface column density dust and gas representative of the diffuse ISM, which will not be reached by the Herschel results. This diffuse ISM may be the most susceptible to the processing effects we intend to study.

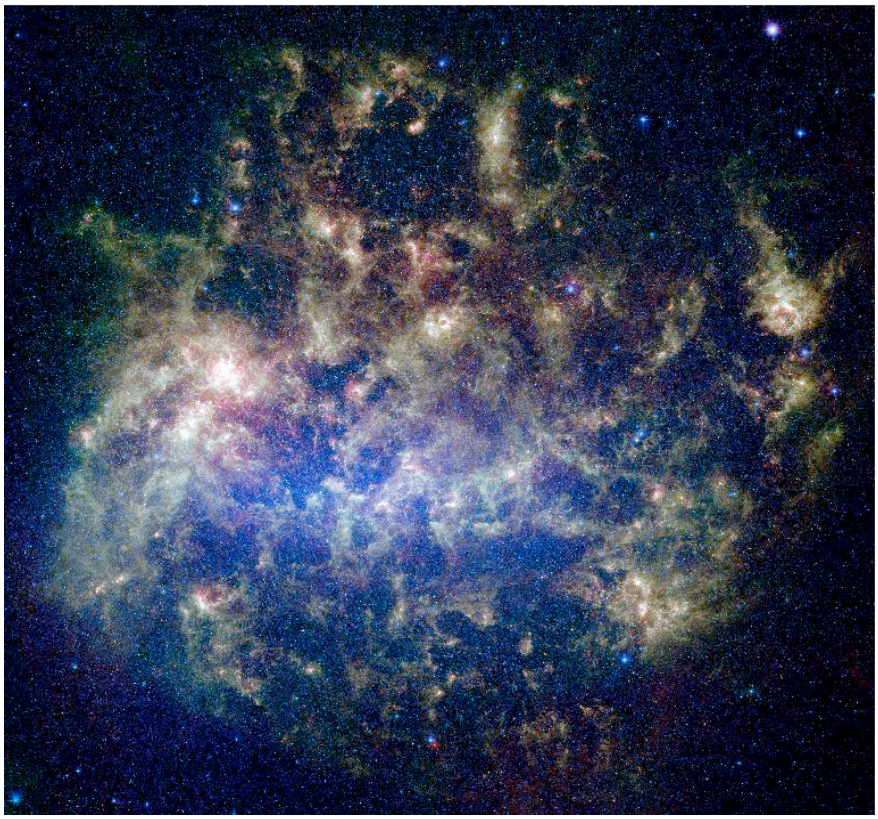

Figure 3.1: Multicolour image of the LMC infrared emission shortwards of 200 microns, obtained by the Spitzer Space Observatory. The very filamentary nature of the dust clouds depicted illustrates their sensitivity to the ambient conditions. A full accounting of dust processing is, however, only possible if the dust emission SED longwards of 20 microns is also carefully determined.

Finally, it should be noted that the program would greatly benefit from any larger aperture, e.g. 25 m. This would allow not so much faster mapping, as indeed deeper mapping. Additional channels at 650 microns and 850 microns would also benefit from an antarctic location, and be especially invaluable in more accurately defining the important submillimeter part of the SED.

3.4 References

Draine B.T., Anderson N, 1985 ApJ 292, 494
Dufour, R., et al, 1982, ApJ, 252, 461
Dumke, M., et al, 2004, A&A, 414, 475
Feast, M., 1999, PASP, 111, 775
Jones A.P, Tielens A.G.G.M., Hollenbach D.J., McKee C.F., 1994 Ap.J. 433, 797
Jones A.P, Tielens A.G.G.M., Hollenbach D.J., 1996 Ap.J. 469, 740
Keller, S.C., & Wood, P. R. 2006, ApJ, 642, 834
L\'eger A., Puget J.L. 1984 A&A 137, L5
Li A., Draine B.T., 2001 ApJ 554, 778
Lisenfeld U., Israel F.P., Stil J.M., Sievers A., 2002 A&A 382, 860
Mathis J.S., Rumpl W., Nordsieck K.H., 1977 ApJ 217, 425
Popescu, C.C., et al, 2002, ApJ, 567, 221
Popescu, C.C., et al, 2002, A&A, 361, 138
Reach, W.T., et al., 1995, ApJ, 451, 188

van der Marel, R., & Cioni, M.-R., 2001, AJ, 122, 1807
van der Marel, R. et al. 2002, AJ, 124, 2639
Weingartner J.C., Draine B.T. 2001 ApJ 548, 296
Whitney, B., et al., 2008, ApJ, in press
Wilke, C.O., et al., 2003, A&A, 401, 873
Zubko V., Dwek E., Arendt R.G., 2004 ApJS 152, 211

4 Galaxy evolution (E. Daddi)

4.1 Galaxy Formation and Evolution, the case for a large telescope operating in the FIR

4.1.1 The need for sensitive FIR observations to map the buildup of stars and black holes

As a result of coordinated observations of the best studied cosmological fields, the broad outlines of the assembly of baryonic matter and its coupling to the cosmic energy budget are starting to emerge. Most of the energy from star formation (SF) and active galactic nuclei (AGN) from high-z is absorbed by dust and re-radiated at infrared wavelengths. Most stars in the universe formed at $1 < z < 4$ (e.g., Dickinson et al. 2003), and the giant black holes (BHs) in the centers of galaxies also grew most of their mass during that period (Hasinger et~al. 2005). The masses of BHs and their host galaxies in the local Universe are closely connected, suggesting co-evolution at high redshift. Current theoretical models invoke the action of AGN to regulate and perhaps terminate SF in massive galaxies (Kaviraj et al. 2007).

However, these processes have only been indirectly studied, and there are few quantitative constraints on the physical mechanisms at work. Nor do we clearly understand high redshift SF. Current measurements of the cosmic SF history over-predict estimates of the stellar mass density at both low and high redshifts (Hopkins & Beacom 2006; Ferguson et al. 2002), suggesting that either the measurements or the stellar population models connecting them are faulty. The mechanisms that govern SF in galaxies are poorly understood: recent evidence points to relatively steady—state growth rather than episodic, merger--driven starbursts, with a tight linkage between galaxy mass and star formation rate (SFR) (Noeske et al. 2007; Elbaz et al. 2007; Daddi et al. 2007a). However, the normalization of this correlation is badly mismatched in theoretical models (Davé et al. 2007). Theory vastly under-predicts the space density of the most rapidly star--forming high-z galaxies (Baugh et~al. 2005), and the evolutionary connection between different high redshift galaxy and AGN populations is poorly understood.

These uncertainties are directly related to the fact that observations to date have only been sensitive to a small fraction of the bolometric energy emerging from dusty SF and AGN. Far-infrared (FIR) measurements have been obtained at wavelengths that are too long (submm) or too short (<100 μm) compared to the emission peak, and have not been sensitive enough to detect typical objects -- only rare, hyperluminous sources have been within reach. Observations of emission from typical star forming galaxies detect only a small fraction of their emergent energy, requiring very large and uncertain extrapolations: either from the ultraviolet (UV), where most young starlight is absorbed by dust, or from mid-infrared (MIR) wavelengths, also subject to large bolometric corrections, where the complexity of spectral emission and absorption features and their underlying physics lead to large uncertainties. A direct view of the thermal emission from galaxies responsible for most of the SF and BH accretion at high redshift has eluded us.

Similarly, most of the background emission at its peak wavelengths (Fig. 4.2, right) is still to be resolved in discrete sources, implying that we have not directly detected yet at these wavelengths a large fraction of the sources responsible for the buildup of stars in the distant Universe. As a result, sensitive observations of the 200-450 μm regions would provide ground breaking new science, allowing to measure the peak of the bolometric emission of distant galaxies (Fig. 4.1, left) and thus to reliably estimate the total energy budget of their powering sources. For star forming galaxies, the

bolometric emission is a direct measure of the ongoing SFR. Accurate measurements of the bolometric emission in galaxies is crucial also to unveil the presence of highly obscured AGN activity, though to be the dominant mode of BH growth at high-z.

4.1.2 Required depths

One can ask, given our current understanding, what is the typical depth that needs to be reached in the FIR in order to address these major scientific questions of the buildup and assembly of stars and supermassive BHs in galaxies, over the 1<z<4 range. Given the existing correlations observed between stellar mass and SFR, evolving in normalization as a function of redshift (Noeske et al. 2007; Elbaz et al. 2007; Daddi et al 2007a, see Fig. 4.2 left), it turns out that reaching to galaxies with typical stellar masses of $\sim 10^{10}$ $M_{\odot}$ is required to obtain a census of most (>2/3) of the stellar mass density and SFR density in the z~2 Universe (Franceschini et al. 2006; Daddi et al. 2007a; Reddy et al 2008). Within this limits, one expects to include also the bulk of obscured AGN activity due to Compton Thick sources (Daddi et al. 2007b; Fiore et al 2008).

This maps into the requirement of measuring bolometric emission of sources having SFR~10 $M_{\odot}$/yr at redshifts up to at least z=3. Reaching such a goal would correspond to ground-breaking progress in the field, and appears within the possibilities of a 12m facility placed at DomeC, given the expected sensitivities (see table 4.1). We estimate that such galaxies would have fluxes of order of 1~mJy at both 350 μm and 450 μm, comparable to the expected confusion limit of the 12m facility at these wavelengths. To compare with the best extragalactic surveys of these days, a GOODS-sized field (150 $arcmin^2$) could be mapped to full depth using a few months of telescope time; a COSMOS-sized area (2 square degrees) would require a full year of telescope exploitation to reach somewhat shallower flux levels of 2-3~mJy (Table 4.1).

4.2 Synergies and complementarity to Herschel and ALMA

Herschel (launch beginning of 2009) will soon explore this 200-450 μm window to unprecedented depths. Its mapping speed at 350 μm and 500 μm with the SPIRE camera will be comparable to that of a 12m facility at Dome C. However, with its 3.5m diameter, Herschel will be very rapidly dominated by confusion noise due to its large beam size, expected to limit surveys to ~15 mJy in these bands. Consequently, only the fairly rare ultraluminous galaxies will be detected at these wavelengths (Fig. 4.1, right). Herschel won't be able to measure directly the bolometric output of typical high-z galaxies. Its shorter wavelengths observations with the PACS camera at 100 and 160$ μm have better resolution and can reach to fainter SFRs (Fig.2, right), but still falling shorter from the necessary dephs by about an order of magnitude for mapping z>2 galaxies. A 12m facility at Dome C would nicely complement Herschel surveys by allowing an order of magnitude depth increase in sensitivity from the bolometric emission of distant galaxies.

ALMA (expected to be in full scale operation by 2015) will allow interferometric imaging down to 450 μm. Thanks to its huge collecting area and exquisite resolution, it is expected to be able to probe to extreme depth down to this wavelength. As a comparison, at fixed observing time ALMA can detect continuum sources 5-10 times fainter than what possible with estimates for a 12m facility at Dome C. However, the primary beam of ALMA antennas at 450 μm is only 9". As result, the mapping speed of a 12m facility at Dome C at 450 μm is 100 times higher. A similar facility will thus be crucial to survey large samples of distant galaxies measuring their bolometric emission to the required faint levels, and to feed ALMA with the best targets for addressing the open problems in galaxy formation and evolution. Even considering the possibility of ALMA surveys at 850 μm or 1.2mm, having larger field of views, and the use of photometry at these wavelengths to indirectly derive the bolometric luminosity, would still imply a 50 times lower mapping speed with respect to a 12m facility at Dome C. This also implies that such a sensitive imaging at 350 and 450 μm will be crucial also to reliably preselect very high-z (z>>4) galaxy candidates for ALMA observations. Having fairly low space densities (<100/deg^2 to

levels probed so far), these sources cannot be easily identified at random by means of deep ALMA pointings.

4.3 SCUBA2 and related surveys

While there is a clear need for such ultradeep FIR observations, which will still be important a decade from now, it is not clear if the required goals can be reached from observational sites other than in Antartica. SCUBA2 at JCMT is claimed to reach comparable NEFD at 450 µm than what estimated here for a 12m facility in Antartica, but these could be reached on relatively rare occasions on Mauna Kea. A survey is planned to cover 1.3 square degree to 2.5 mJy depth at 450 µm. These goals might be over optimistic, so far observations from Mauna Kea at these wavelengths have not pushed significantly below 20 mJy.

4.4 A case for a much larger facility ?

To match Herschel's confusion limit at 160 µm with 200 µm observations with a 12m facility at Dome C would require ~100 hours. To beat Herschel at 200 µm and competitively exploit that window requires a 25m telescope. We emphasize the gigantic leap forward that would be enabled from a 25m telescope (single dish or interferometer): the mapping speed would grow by D^2 (a factor of 4). Even more importantly for extragalactic surveys where the sensitivity is still the major limiting factor, the time to reach a given flux would go down as D^4 (a factor of 16). The much smaller PSF would virtually solve all confusion issues for extragalactic deep fields.

4.5 Accessing the best studied fields

A facility in Antartica could not access some of the currently best studied cosmological field that are either equatorial or in the Northern emisphere. However, it could access southern fields that could be observed in sinergies with ALMA and existing Southern facilities (Chile, South Africa, Australia). Deep fields in the southern emisphere already exists (notably, the Hubble Deep Field South and flankign fields, the GOODS-South and Extended CDFS field, the "Marano field").

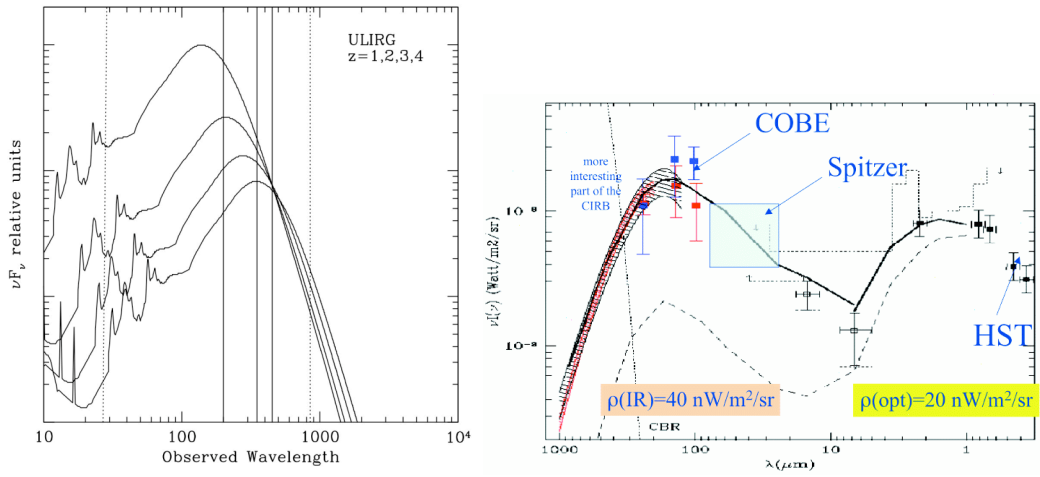

Figure 4.1. **Left**: Spectral energy distribution of Ultraluminous IR galaxies (ULIRGs), redshifted at z=1,2,3,4. The peak of the bolometric emission shifts at 200-400 µm as a function of redshifts, well centered to the wavelengths accessible at DomeC. The dotted vertical lines show the 24 µm (Spitzer) and 850 µm (Scuba, etc) observing wavelengths. **Right**: a recent determination of the extragalactic background light, as a function of wavelength (Franceschini et al 2008). The FIR portion accounts for the largest fraction of the background, and peaks between 100-300 µm. The background at >200 µm is dominated by distant, cosmological sources and thanks to K-correction effects it is a direct tracer of star formation in the distant Universe.

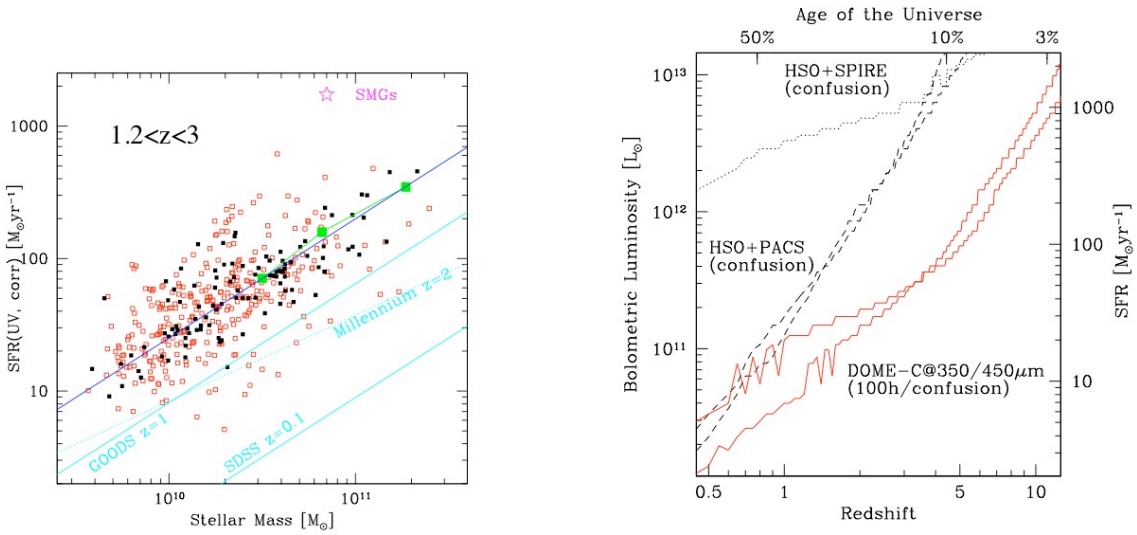

Figure 4.2. **Left**: The correlation between stellar mass and SFR in z~2 galaxies (adapted from Daddi et al 2007a). **Right**: Limiting depths for star forming galaxies that can be reached with Herschel PACS and SPIRE imaging to their respective confusion limits, compared to that of 350 μm+450μm observations from a 12m facility at Dome C (100 hours of observations of a deep field, mapping 40 arcmin^2 down to ~1 mJy at both wavelengths). Flux limits are converted to corresponding bolometric luminosities using the Chary & Elbaz (2001) template libraries.

Table 4.1: Extragalactic survey speed: censing galaxy and black hole mass assembly. We assume coadding 350 μm and 450 μm data for maximum efficiency. SFR limits are for a Salpeter IMF, computed using the Chary & Elbaz 2001 library. Facility speed is estimated assuming 50% of usable time per year and 50% of operational overhead.

Integration (per field)	5 sigma limit (point source)	SFR(z=2) $M_\odot$/yr	SFR(z=4) $M_\odot$/yr	Facility speed deg per yr
100 h	1 mJy	~20	70	0.2
10 h	2.5mJy	~70	~200	2.0

5 Far-infrared and submillimeter spectroscopy of galaxies along their evolution (L. Spinoglio)

5.1 What is the science goal

One of the most important astrophysical questions that still has to be ansewered is *how galaxies evolve from the first structures to the present day*. A great effort has been done with the cosmological surveys of ISO and Spitzer and with ground-based submillimeter telescopes (eg the SCUBA surveys at JCMT). In the incoming years, Herschel will continue this work with the large amount of time devoted to deep and shallow surveys. The approach is to observe deep fields in a few photometric bands to derive the logN-logS distributions, build the spectral energy distributions to be used -together with models- to distinguish among the various types of galaxies (spheroids, ellipticals, starburst or AGN) at different redshifts. Follow up spectroscopic work from large optical and near-IR ground-based telescopes can give more accurate redshifts. The limitation of this approach is however the lack of detailed information on the physical processes dominating the energy budget, that makes any conclusion on the nature of the observed objects very model dependent. Only spectroscopic surveys at different redshift, at the wavelengths where the bulk of the energy is emitted (mid-to-far infrared) will be able to identify the energy production mechanisms during their evolution and therefore their nature. This will shed light into the role of AGNs and starbursts along galaxy evolution.

We already know that the main energy-generating mechanisms in galaxies are black hole accretion and star formation and that starbursts and AGNs may be linked in an evolutionary sequence. In the last decade it became more and more evident: the black hole mass correlates with the bulge luminosity (Kormendy and Richstone 1995) and with the mass of the bulge (Magorrian et al 1998; Haring & Rix; Marconi & Hunt 2003). Moreover the black-hole mass also corelates with the stellar velocity dispersion in the galactic bulges of galaxies (Ferrarese and Merrit 2000; Shen et al 2008). It appears therefore that the formation of spheroids (at the origin of bulges) is linked to the growth of the Black Holes.

On a cosmic scale, the evolution of supermassive black holes appears tied to the evolution of the star-formation rate (Marconi et al 2004; Merloni et al 2004). Heckman et al (2004) concludes a study of 23,000 low-redshift narrow emission-line AGNs of the Sloan Survey, suggesting that *the growth of black holes through accretion* and *the growth of bulges through star formation are related at the present time in the same way that they have been related, on average, throughout cosmic history.* Also on a local scale *star formation* and *nuclear activity* are linked. The possible evolutionary scenario is: HII galaxies → Seyfert type2 (Storchi-Bergmann et al 2001; Kauffmann et al 2003), or extended to: HII galaxies → Seyfert 2's → Seyfert 1's (Hunt & Malkan 1999; Levenson et al 2001; Krongold et al 2002). In this scheme, starburst emission is first triggered by galaxy interactions, leading to the concentration of a large gas mass in the circumnuclear region of a galaxy. Later, mergers and bar-induced inflows can bring fuel to a central black hole, stimulating AGN activity.

Given the above scenario, the scientific aim that we want to reach is to understand galaxy evolution through the history of the luminosity source of galaxies. The observational approach is based on mid-to-far IR and submillimeter spectroscopy, able to the derive the bi-variate AGN and Star Formation luminosity functions at various cosmic epochs, from the Local Universe to high redshifts. The spectroscopic diagnostics will include the typical AGN tracers (high ionization lines) and star formation tracers (HII regions lines and low-ionization or neutral lines, such as the [OI] and [CII] far-IR transitions). This observational goal can be reached at Dome C with a large (12m) submillimeter telescope, operated in the submillimeter windows in particular at 200μm, 230μm and 280μm - which open only at Dome C when the precipitable water vapor (PWV) content of the atmosphere reaches levels of the order of 0.1-0.2mm. At these low levels of PWV also the mid-IR (in the range of 10-40μm) atmospheric windows open and mid-IR observations can be collected, provided that the submillimeter telescope has an inner part (3-4m) of its mirror optically worked. This dual channel observatory will collect imaging and spectroscopic data with comparable beam sizes at 10-40μm and 200-350μm of galaxies at increasing redshifts.

5.2 What are the spectroscopic tracers

Mid-IR and submillimeter spectroscopy can trace both the AGN (photoionization from non-thermal processes) and the Star Formation component (stellar photoionization, shocks, PDRs - photodissociated regions), not suffering extinction that obscures the galactic nuclei both locally and at cosmic times. Moreover, in this spectral range fine-structure emission lines can be used as tracers of the physical conditions in galaxies from the local universe to distant cosmological objects.

Fig. 5.1 shows the very large density-ionization plane that can be traced by infrared fine-structure lines, which are good diagnostics for gas densities of $10^2 \rightarrow 10^8$ cm^{-3} and ionization potentials up to 350 eV. The critical density (i.e. the density for which the rates of collisional and radiative de-excitation are equal) of each line is plotted as a function of the ionization potential of its ionic species. This diagram shows how these lines can measure the two fundamental quantities (density and ionization) of the gas. Lines from different emission regions are shown in different loci. The ratio of two lines with similar critical density, but different ionization potential, measures the ionization, while the ratio of lines with similar ionization potential, but with different critical density, can measure the density of the gas (see eg: Spinoglio & Malkan 1992). The identified emission line regions span from neutral or weakly ionized regions, such as PDR at the interface between HII regions and molecular clouds, HII regions excited by young stars, Narrow Line Regions excited by the AGN and the so-called Coronal Line

Regions with the highest ionization lines, originated from the high energy photons emitted during the AGN accretion process.

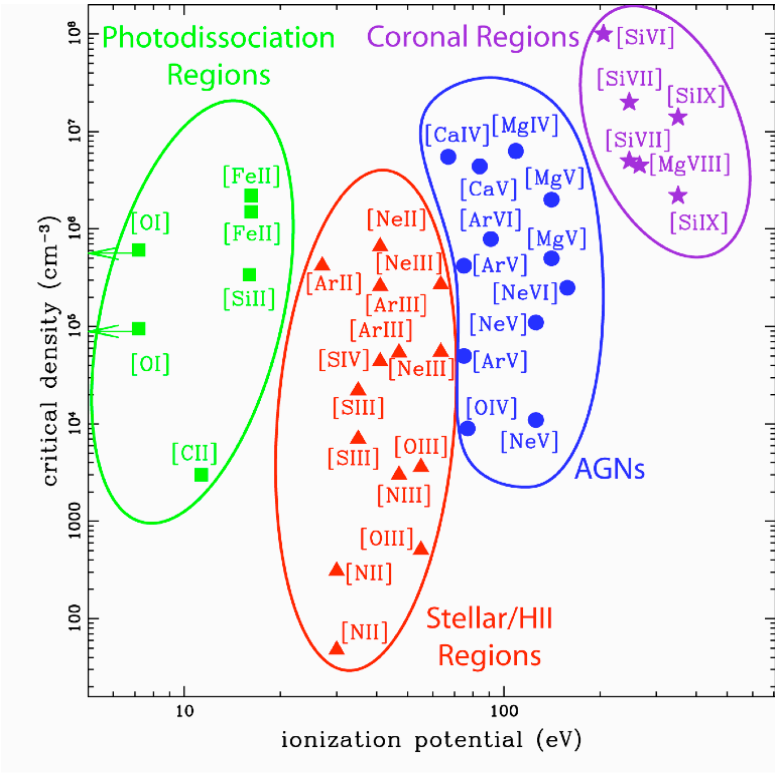

Figure 5.1 Fine-structure lines in the 3-200 μm range. The lines are plotted as a function of their ionization potential and critical density. Different areas are identified for lines from photodissociation regions, stellar/HII region lines, AGN lines and coronal lines.

5.3 What are the lines in the atmospheric windows at Dome C

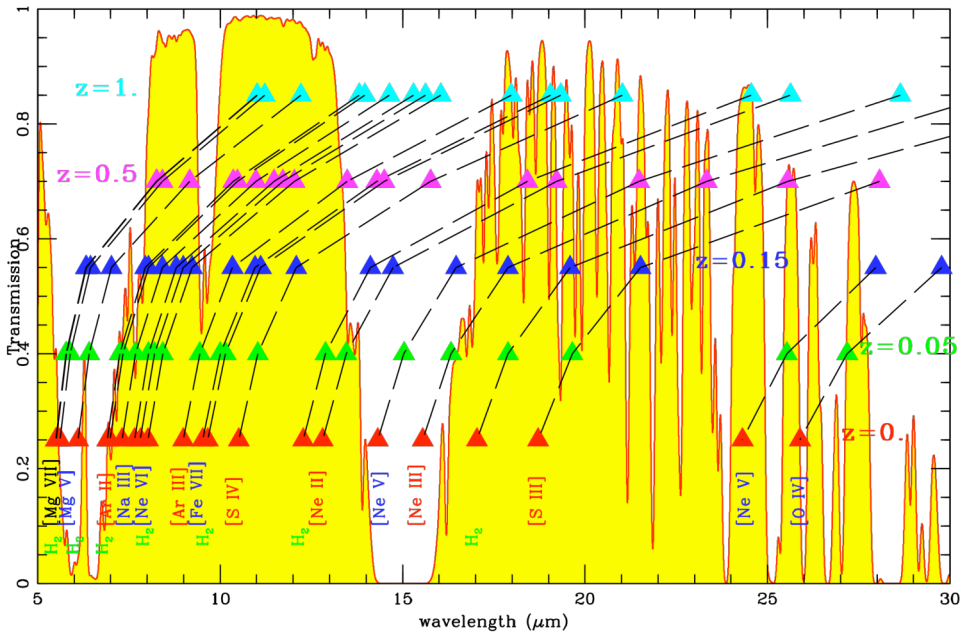

Figure 5.2 5-30μm transmission curve at Mauna Kea with PWV=1mm. Some of the wavelengths of fine structure lines and the H_2 rotational lines are marked for different values of the redshift (z=0., 0.05, 0.15, 0.5 and 1.), showing many transitions accessible from the ground.

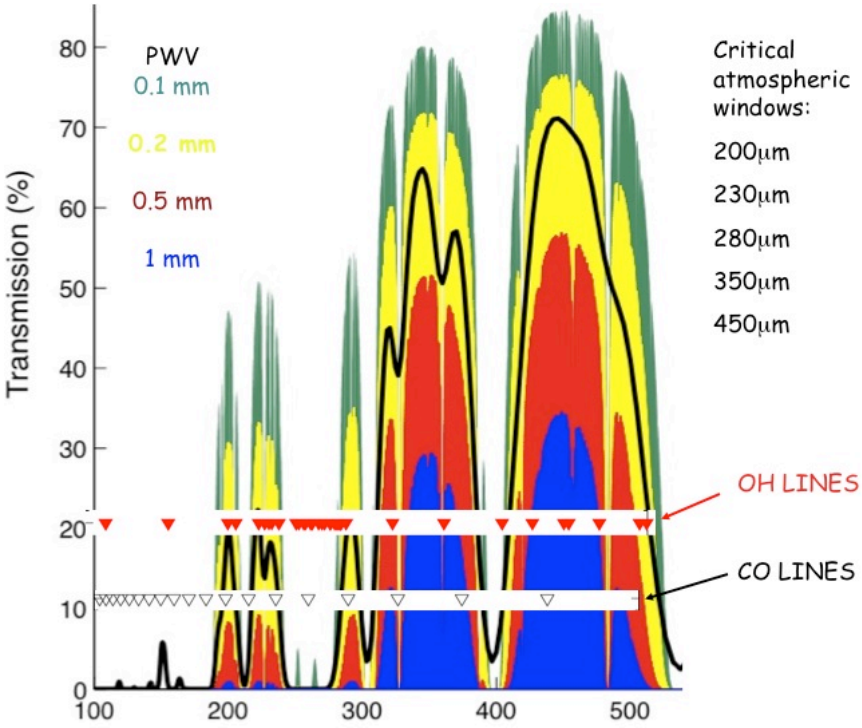

Figure 5.3 Submillimeter atmospheric windows for different values of the PWV. Important CO and OH lines lie in the atmospheric windows.

5.4 What are the expected lines intensities

Considering the three local galaxies M82, NGC1068 and NGC6240 as template objects, we computed the line intensities expected at redshifts ranging from 0.1 to 5. For simplicity, we adopted an Einstein-De Sitter model Universe, with $\Omega_\Lambda = \Omega_{vac}=0$ and $\Omega_M= 1$, Ho=75 km s^{-1} Mpc^{-1}. The luminosity distances have been derived using: $d_L(z)= (2c/Ho) [1+z - \sqrt{(1+z)}]$.

The results are reported in Fig. 5.4, where the line intensities are given in W m^{-2} and the expected sensitivities of the Herschel PACS spectrometer are reported. We have assumed that the line luminosities scale as the bolometric luminosity a luminosity evolution proportional to the $(z+1)^2$, consistent with the Spitzer results at least up to redshift z=2 (Perez-Gonzalez et al. 2005).

References

Ferrarese and Merrit 2000, ApJ, 539, L9
Haring & Rix, 2004, ApJ, 604, L89
Hunt & Malkan 1999, ApJ, 516, 660
Kauffmann et al 2003, MNRAS, 346, 1055
Kormendy and Richstone 1995, ARAA, 33, 518
Krongold et al 2002, ApJ, 572, 169
Levenson et al 2001, ApJ, 550, 230
Magorrian et al 1998, AJ, 115, 2285
Marconi et al 2004, MNRAS, 351, 169
Marconi & Hunt 2003, ApJ, 589, L21
Merloni et al 2004, MNRAS, 354, 37
Heckman et al 2004, ApJ, 613, 109

Shen et al 2008, AJ, 135, 928
Spinoglio & Malkan 1992, ApJ, 399, 504
Storchi-Bergmann et al 2001, ApJ, 559, 147

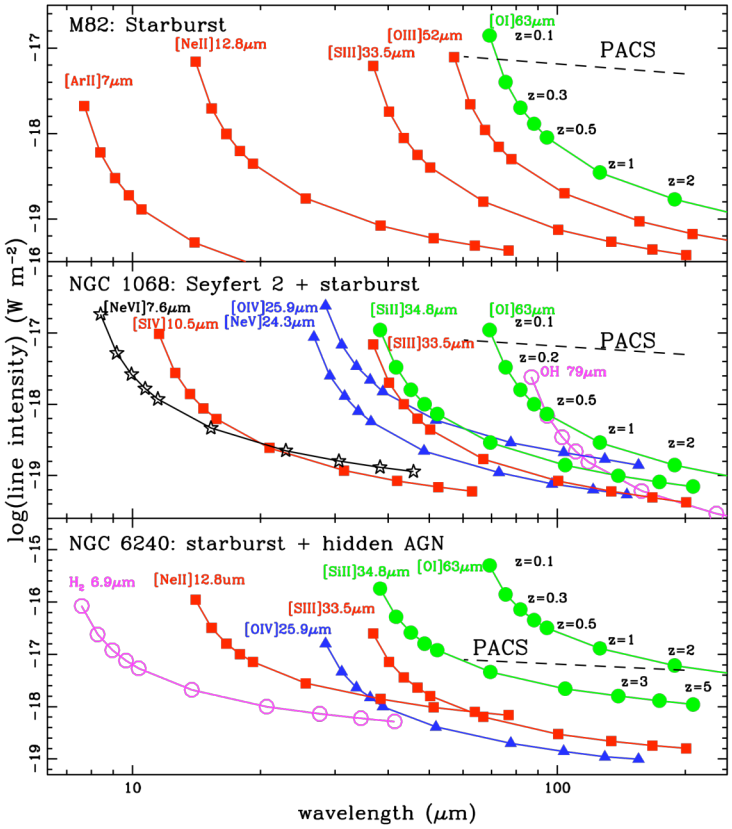

Figure 5.4 Predicted line fluxes as a function of redshift, using three local templates. Squares indicate the fluxes of HII region lines, triangles the fluxes of lines emitted by AGN, filled circles the fluxes of the [OI] and [SiII] lines and open circles molecular lines (from OH and H_2).

6 A potential case for Dome C: the Sunyaev-Zel'dovich Effect (M. de Petris)

6.1 Introduction

A large amount of information in Cosmology has been derived, and is still under analysis, through observations of the primary anisotropies of the Cosmic Microwave Background (CMB), the tiny fluctuactions in temperature, reflecting the density ones, present at the epoch of transition when CMB photons decoupled by neutral matter at redshift ~1100. The energy/matter budget of the universe has been partitioned in a 5% of baryonic matter, a 25% of dark matter and a remaining of 70% of dark energy to allow a flat universe with a present density close to the critical one, as it results from observations [de Bernardis et al. 2002, Komatsu et al. 2008].

A promising science, that is having by right a key role in the so called Precision Cosmology Era, is the study of the secondary anisotropies of the CMB. We observe today the CMB photons as they left the last scattering surface but after travelling to us and so interacting with all the matter along their path through the universe. These interactions have generated the secondary anisotropies that we can discriminate on the basis of the two main families of matter & radiation interactions: by gravitational potential wells and by scattering. We focus on one of the second family.

The Sunyaev-Zel'dovich Effect (SZE) is the distortion induced into the CMB spectrum by the energy transfer due to Thomson scattering of CMB photons by hot gas. The observed anisotropy is at the scale of galaxy clusters and superclusters, even if it may also be produced on very small scales by the first stars in the universe [Sunyaev & Zel'dovich 1972, 1980; Rephaeli 1995, Birkinshaw 1999, Carlstrom, Holder & Reese 2002]. The SZE is known as a nuisance factor to cosmological parameter extraction from measurements of primary CMB anisotropies, but it is a potentially powerful tool for cosmology. Accurate spectral and spatial observations makes the SZE a *radial speedometer* and an efficient *mass finder* both in a direct way for baryonic matter (visible or dark), and in an indirect way for non baryonic dark matter. The peculiar independence of this effect from the redshift of the scattering source allows observations of far away targets avoiding the brightness reduction present in visible and X-ray spectral ranges surveys.

The thermal component (th-SZE) is a CMB spectral distortion due to the inverse Compton interaction between the CMB photons and free electrons of a hot ionised gas along the line of sight. The result is a net energy transfer from photons in the Rayleigh-Jeans tail of the CMB spectrum to the Wien tail. The cross-over frequency, corresponding to a null distortion, is around 217 GHz but a weak dependence of this value on the gas temperature is also present.

The kinetic Sunyaev-Zel'dovich Effect (k-SZE) is the component due to the Doppler effect caused by the bulk motion of the electron gas that scatters the CMB photons. In the non-relativistic regime it causes no spectral distortion, maintaining a planckian spectrum, therefore resulting a challenging detection because it is impossible to disentangle from primary CMB anisotropy at the same angular scales. In the case of angular scales corresponding to multipole index larger than $\mathbf{l} \geq 2500$ (*i.e.* $\theta \leq 5$ arcminutes) SZE components dominate CMB fluctuations as shown in Fig.6.1.

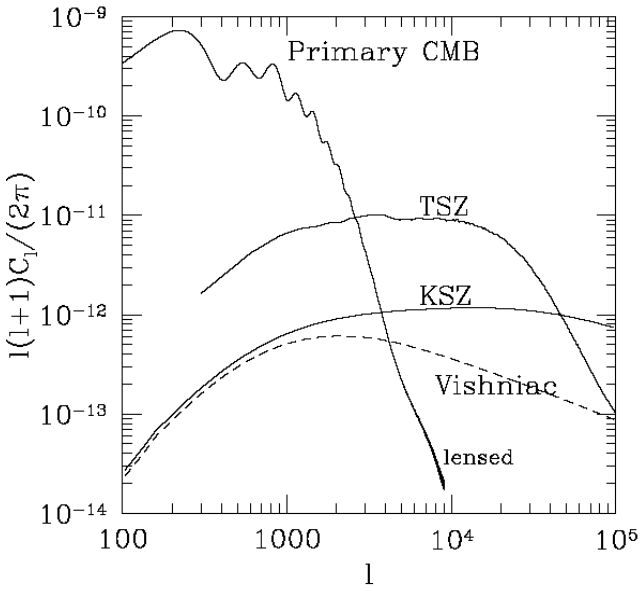

Figure 6.1 - Thermal and kinetic SZE power spectra as deduced by numerical simulations compared with CMB power spectrum. The results include non-linear regime and are obtained by assuming universe was reionised at z = 16.5 and remained ionised after that [Zhang, Pen & Trac , 2004].

Relativistic corrections have to be considered in the presence of hotter and denser scattering media [Itoh et al. 2002; Shimon & Rephaeli 2002]. Non-thermal populations of electrons can also contribute as a different components to the SZ spectrum [Colafrancesco, Marchegiani & Palladino 2003]. The main components of SZE are shown in Fig.6.2 with the expected atmospheric windows from Dome C assuming optimum observational conditions with a pwv equals to 0.1mm.

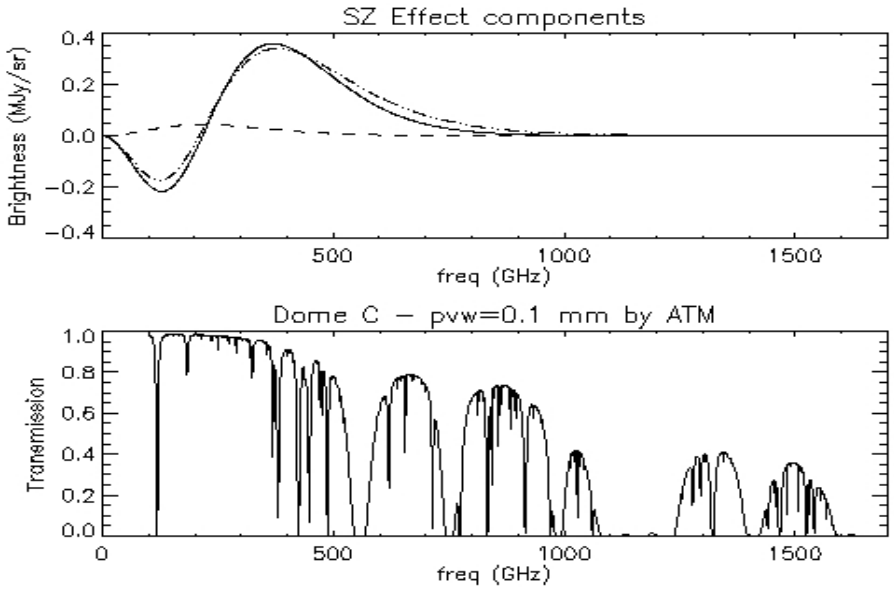

Figure 6.2 – *Upper panel*: SZE spectra splitted in thermal component (solid line), kinetic component (dashed line) and all the components with relativistic corrections (dot-dashed line). *Lower panel*: transmission at Dome C as derived by ATM programme considering a precipitable water value equals to 0.1mm.

The SZE is mainly caused by the pressure of free electrons of hot ionised gas entailing that intracluster gas (IC) is the most favourite ambient. In this way SZE blind surveys allow to count all the clusters of galaxies which do not exhibit an alternative visible counterpart. Having the instrumental capability to detect high redshift clusters (*i.e.* sensitivity and angular resolution) gives the possibility to reconstruct the evolution of this structures allowing to put constraints to cosmological parameters such as the amount of dark energy and its equation of state (see Fig.6.3).

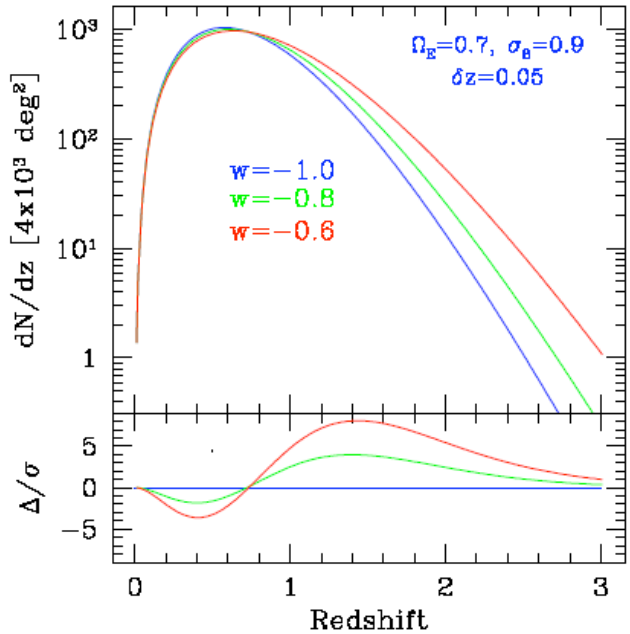

Figure 6.3 – The cluster redshift distribution for a 4000 deg^2 SZE survey proposed for the South Pole is sensitive to the dark energy equation of state w. Three models with different w are shown (above) and statistical differences quantified (below) [Mohr 2005]

Anyway we have to highlight that SZE takes place in all astrophysical environments where both the conditions of ionisation and high temperature are fulfilled at the same time. Hydrodynamical simulations show that diffuse matter in the phase of warm-hot gas (T_e=$10^5$4$10^7$ keV) is expected to be present in large structures in the form of filaments. This gas might account for a fraction of the

missing baryons in the universe [Fukugita, Hogan & Peebles 1998]. The th-SZE of this gas is really low and comparable to the k-SZE component; even if the SZE luminosity is low this is a valid alternative for searching missing baryons.

An interesting scientific goal derived by SZE observations is the extraction, together with other cluster parameters, of the temperature of the CMB photons at cluster redshift allowing the monitoring of the CMB temperature evolution [see Battistelli et al. 2002 for the first observational approach].

Targets for SZE can be distinguished between observations of individual clusters, in order to collect a large sample of them, and wide blind surveys for statistical approaches.
The expected results can be summarised as in the following:

- reconstruction of the Hubble diagram for deriving cosmological parameters;
- counting clusters along the redshift for deriving cosmological parameters;
- estimate of baryon mass fraction;
- measuring CMB temperature along the Universe.

More challenging results are:

- detection of missing baryons;
- mapping of radial peculiar velocities of galaxy clusters for constraining dark energy parameters.

6.2 Peculiarities for Dome C SZE observations

The site allows observational conditions common with other scientific objectives; mainly resulting in excellent measurement conditions for the mm-FIR spectral range from ground. The possibility of performing simultaneous observations in all atmospheric windows between 200 μm and 2 mm allows deep integration towards sky regions with high angular resolution and large spectral coverage.

FWHM=BT (arcmin)	δT_{rms} (μK)	$\lvert v_{min}\rvert$ (km/s)
0.1	2.1	46
0.2	4.2	93
0.3	6.3	138
0.4	8.3	184
0.5	10.3	227
1	19.4	426
2	32.2	708
3	39.6	871
4	44.1	969
5	46.9	1033
6	49.1	1079
7	50.8	1117
8	52.2	1149
9	53.4	1175
10	54.4	1196

Table 6.1 – Estimated CMB temperature dispersion considering a double beam differential sky observations with a beamthrow (BT) equals to the field of view (FWHM). The correspondent cluster peculiar velocity along the line of sight is converted assuming an electronic optical depth equals to $5 \cdot 10^{-3}$.

The SZE spectrum does not show spectral features demanding high spectral resolution and so the possibility of observation by multi-frequency photometers or by spectrophotometers is allowed.

A large dish telescope (12-m or more in diameter) allows the possibility to carefully explore far away Universe looking for clusters of galaxies by blind surveys. An high angular resolution, difficult to

reach by a satellite instrument, (*i.e.* fov=24" FWHM @ 1.4mm, the cross-over wavelength) ensures an accurate mapping of the morphology of large clusters. A reduced contamination by primary CMB anisotropies opens the exploration of k-SZE observations. See in Tab.6.1 the reduction of CMB confusion, converted also in the minimum detectable cluster peculiar velocity, as decrease the field of view (FWHM). A double beam differential sky observations are considered with a beam-throw BT equals to the fov.

A multi-frequency observation of the full SZE is mandatory for an efficient extraction of gas parameters: electrons density and temperature and cluster radial peculiar velocity. For this purpose extending the observations to high frequencies allow to sample the intracluster dust emission disentangling this contamination from SZE spectra at low frequencies.

An accurate forecast of confusion by mm/FIR point sources is requested. It is often pointed out that mm/submm surveys may suffer from strong confusion limits due to the tail of IR emission from unresolved compact objects (active galaxies and spheroids). A precise evaluation of these confusion limits is therefore critical to fully assess the capabilities of a facility to operate at given wavelengths in presence of strong contaminating fluxes integrated on its field of view. This evaluation is dependent on the assumed model for the source distribution (with special regard to the clustering phenomena) and, of course, on the limits set by the angular resolution of the telescope [Lapi et al. 2006; De Zotti et al. 2005; Negrello et al. 2007]. In Table 6.2, we show the scaling of the confusion limits for reference microwave frequencies observable from the ground, for a well assessed source distribution model, as a function of the telescope aperture. It is clear that the choice of large aperture telescope like the proposed 12m facility from Dome C can provide a significant leap forward in SZ science by providing smaller levels of spurious contamination from unresolved compact objects.

frequency (GHz)	1σ confusion limit (mJy)
140	0.46
217	0.63
270	0.84
350	1.00

Table 6.2 – Confusion limits at low frequency bands assuming a diffraction limited field of view for a 12-m in diameter telescope aperture.

Accurate predictions about the results and the observational strategy can be provided when a dedicated focal plane instrumentation will be planned: *i.e.* mm/sub-mm spectrophotometer with imaging capabilities.

References

Battistelli, E.S., De Petris, M., Lamagna, L. et al., ApJL, 580, 101, (2002)
Birkinshaw M., Physics Reports, 310, 97, (1999)
Carlstrom J.E., Holder G.P. & Reese E.D., ARA&A, 40, 643, (2002)
Colafrancesco S., Marchigiani P. & Palladino E., A&A, 397, 27, (2003)
de Bernardis P. et al. Ap. J. 564, 559 (2002)
De Zotti et al. A&A (2005)
Fukugita M., Hogan C.J. & Peebles P.J.E., Ap.J. 503, 518 (1998)
Itoh N. et al. A&A, 382, 722 (2002)
Lapi et al. (2006)
Komatsu E. et al., arXiv:0803.0547v1(2008)
Mohr JJ.. *Astron. Soc. Pac. Conf. Ser.*, 339: 140. Astron. Soc. Pac. (2005)
Negrello et al. MNRAS (2007)
Rephaeli Y., Ap.J., 445, 33, (1995)
Shimon M. & Rephaeli Y., ApJ, 575, 12, (2002)

Sunyaev R.A. & Zel'dovich Ya.B., Comm. Astrophys. Space Phys., 4, 173, (1972)
Sunyaev R.A. & Zel'dovich Ya.B., ARA&A, 18, 537, (1980)
Zhang P., Pen U.L. & Trac H. , MNRAS, 347, 1224 (2004)

7 Unique science case: Understanding Sun coronal mass ejection (V. Minier)

7.1 Impact

Synchrotron radiations are emitted during Sun coronal mass ejections and are usually observed in the microwave part of the spectrum. Understanding this phenomenon will shed light on the physical mechanisms that are responsible for coronal mass ejections such as particle acceleration from the photosphere.

Recent results obtained at submm wavelengths have revealed another potential synchrotron radiation spectrum (Fig. 7.2; Kaufmann et al. 2004). This new spectral component discovered with fluxes increasing for shorter submillimeter wavelengths may indicate that the submm emission is created by particles accelerated to very high energies.

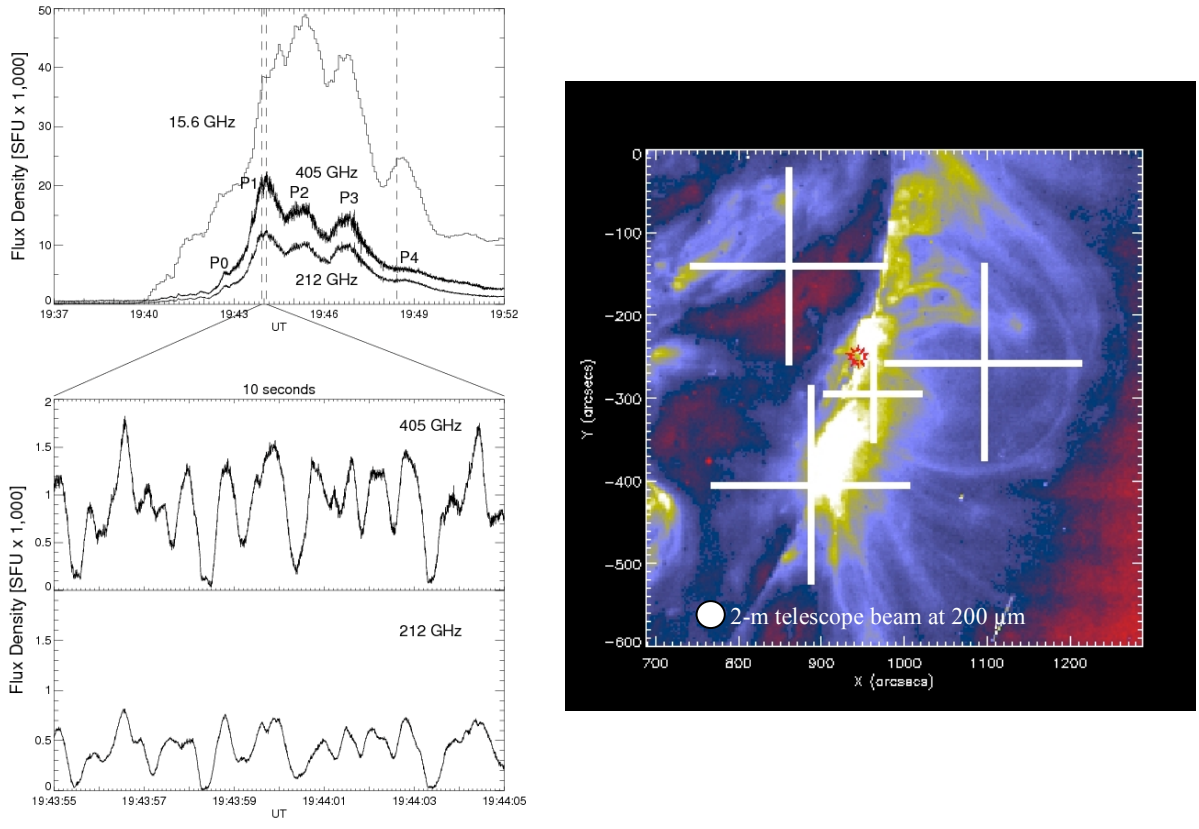

Figure 7.1: Left : Time profiles of the Solar burst in November 2003. The 405-GHz emission is more intense than the 212-GHz emission, suggesting a possible maximum in the submm/far-infrared domain. Right : Position of the submm observing beam on the SOHO UV image of the Sun. (from Kaufmann et al. 2004).

First emission models assume three different mechanisms which may become comparable in importance: (a) synchrotron radiation by beams of ultrarelativistic electrons; (b) synchrotron radiation by positrons produced by nuclear reactions arising from energetic beams interactions at dense regions close to the photosphere, and (c) Langmuir waves emission from deep photosphere excited by high energy electron beams (Kaufmann et al. 2006).

Overall, these new results indicate that key questions regarding the physical mechanisms at the origin of solar flares are expected to become better understood with measurements in the far to mid-infrared range.

7.2 Other facilities

The Solar Submillimetre-wave Telescope (SST) is located in Argentina at an altitude of 2550m. It is a 1.5m-diameter Cassegrain telescope that can observe at 212 and 405 GHz, which convert to 1.5 mm and 750 µm, respectively. The FWHM beams are 2 and 4 arcmin in these two respective channels. Observations of the Sun require good atmospheric conditions at 2550m despite the large Solar flux density in the submm (>10,000 Jy) because the atmosphere may become opaque at these wavelenghts. Observations with SST have revealed submm bursts in the Solar corona that were associated to the large solar flares in November 2003 (Fig. 7.1).

The current limitation of the SST is the quality of the atmosphere and the corresponding transmission. Observations at 200 µm are basically impossible from the SST site in Argentina. Observations from 500 µm down to mid-IR are important to understand whether incoherent synchrotron radiations are the main mechanisms that generate submm flares (Fig. 7.2). Space is an option with instrument operating at both 150 and 35 µm (e.g. SMESE/DESIR project) but it will be limited in time and in sensitivity. The SMESE bolometers will not be cryogenically cool down. Only major flares with respect to the thermal emission of the Sun will be detected. A second limitation of SST is its size that does not allow high angular resolution observations on the Sun (<1 arcmin).

Another option is a 2-m class telescope at Dome C in Antarctica. It could operate at both 30 and 200 µm. Given the large flux of the Sun at these wavelengths, observations during day time with only PWV=0.3 mm should be possible. Cryogenically cooled detectors should allow detection of minor flares in intensity. Secondly, a 2-m class would offer a better angular resolution to disentangle the potential sources of flares on the Sun (see Fig. 7.2). A higher angular resolution, and therefore a larger telescope than 2 m in diameter, is not necessary for observing the Sun.

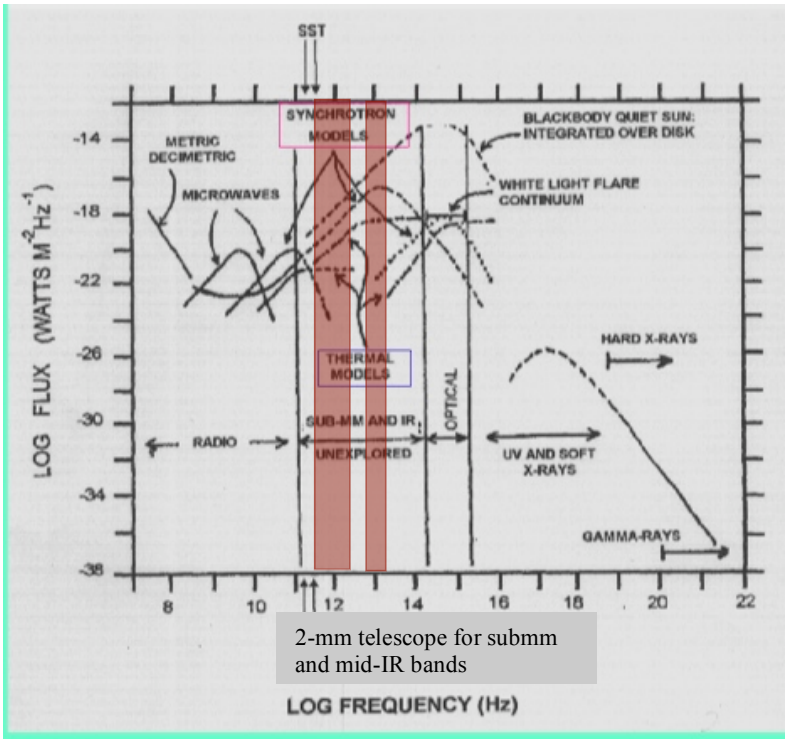

2-mm telescope for submm and mid-IR bands

Figure 7.2 : Spectral energy distribution of Sun emission. Synchrotron radiations from the Sun are expected in microwave, submm and infrared domains. Incoherent synchrotron radiations are predicted in the submm and mid-infrared at wavelengths observable with a 2-m class telescope (red stripes).

7.3 Observations and requirements

To perform submm observations of the Sun, we propose to install a 1000-pixel bolometer array on a 2-m class telescope that could operate at both 200 or/and 350 µm. It could be used either on a monitoring mode or as a follow-up imager if a flare is detected in the visible and UV.

Complementary observations in the mid-infrared would also constrain the spectral energy distribution of the incoherent synchrotron radiation. A 2-m class telescope as Sun corona mass ejection observer will be highly complementary to the Murchison Widefield Array (MWA) in Western Australia whose main goal is to constrain the magnetic field strength during Sun coronal mass ejections.

Special optical filters or shield should be installed in front of the telescope or across the dome aperture for observing the Sun in the submm with a 2-m class telescope.